

2

GL-TR-90-0124  
ENVIRONMENTAL RESEARCH PAPERS, NO. 1062

# AD-A229 920

## WADOCT—An Atmospheric Dispersion Model for Complex Terrain

BRUCE A. KUNKEL  
YUTAKA IZUMI

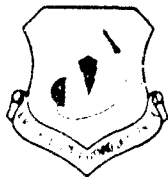
DTIC  
ELECTE  
DEC 13 1990  
S D D  
D G



9 May 1990



Approved for public release; distribution unlimited.



20030206195



ATMOSPHERIC SCIENCES DIVISION PROJECT 6670  
**GEOPHYSICS LABORATORY**  
WANS COM AFB, MA 01731-5000

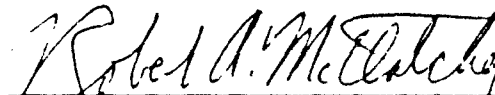
This report has been reviewed by the ESD Public Affairs Office (PA) and is releasable to the National Technical Information Service (NTIS).

"This technical report has been reviewed and is approved for publication"

FOR THE COMMANDER



DONALD D. GRANTHAM  
Chief, Atmospheric Structure Branch



ROBERT A. McCLATCHEY  
Director, Atmospheric Sciences Division

Qualified requestors may obtain additional copies from the Defense Technical Information Center. All others should apply to the National Technical Information Service.

If your address has changed, or if you wish to be removed from the mailing list, or if the addressee is no longer employed by your organization, please notify AFGL/DAA, Hanscom AFB, MA 01731. This will assist us in maintaining a current mailing list.

Do not return copies of this report unless contractual obligations or notices on a specific document requires that it be returned.

# REPORT DOCUMENTATION PAGE

Form Approved  
OMB No. 0704-0188

Public reporting burden for this collection of information is estimated to average 1 hour per response, including the time for reviewing instructions, searching existing data sources, gathering and maintaining the data needed, and completing and reviewing the collection of information. Send comments regarding this burden estimate or any other aspect of this collection of information, including suggestions for reducing this burden, to Washington Headquarters Services, Directorate for Information Operations and Reports, 1215 Jefferson Davis Highway, Suite 1204, Arlington, VA 22202-4302, and to the Office of Management and Budget, Paperwork Reduction Project (0704-0188), Washington, DC 20503.

<b>1. AGENCY USE ONLY (Leave blank)</b>		<b>2. REPORT DATE</b> 9 May 1990	<b>3. REPORT TYPE AND DATES COVERED</b> Scientific Interim May 89-May 90	
<b>4. TITLE AND SUBTITLE</b> WADOCT—An Atmospheric Dispersion Model for Complex Terrain			<b>5. FUNDING NUMBERS</b> PE-62101F PR-6670 TA 14 WU 09	
<b>6. AUTHOR(S)</b> Bruce A. Kunkel Yutaka Izumi				
<b>7. PERFORMING ORGANIZATION NAME(S) AND ADDRESS(ES)</b> Geophysics Laboratory/LYA Hanscom AFB Massachusetts 01731-5000			<b>8. PERFORMING ORGANIZATION REPORT NUMBER</b> GL-TR-90-0124 ERP, No. 1062	
<b>9. SPONSORING/MONITORING AGENCY NAME(S) AND ADDRESS(ES)</b>			<b>10. SPONSORING/MONITORING AGENCY REPORT NUMBER</b>	
<b>11. SUPPLEMENTARY NOTES</b>				
<b>12a. DISTRIBUTION/AVAILABILITY STATEMENT</b> Approved for Public Release; Distribution Unlimited			<b>12b. DISTRIBUTION CODE</b>	
<b>13. ABSTRACT (Maximum 200 words)</b> WADOCT (Wind and Diffusion Over Complex Terrain) is a complex terrain dispersion model capable of running on a microcomputer. It consists of two models: 1) AFWIND, a surface-layer windflow model, and 2) AFTOX, a Gaussian puff dispersion model. The terrain induced wind field and the dispersion pattern are computed separately and independently of each other. Through a transformation scheme the location and shape of the plume footprint is then adjusted to the computed wind field. An evaluation of the model is presented using data from the AMALEUS and the Mountain Iron dispersion experiments. The evaluation shows that the model tends to underpredict the adjustment to the wind direction and overpredict the length and width of the plume footprint.				
<b>14. SUBJECT TERMS</b> Atmospheric dispersion, Air pollution, Wind model Toxic chemical dispersion, Chemical hazard. (200) ←			<b>15. NUMBER OF PAGES</b> 52	
			<b>16. PRICE CODE</b>	
<b>17. SECURITY CLASSIFICATION OF REPORT</b> Unclassified	<b>18. SECURITY CLASSIFICATION OF THIS PAGE</b> Unclassified	<b>19. SECURITY CLASSIFICATION OF ABSTRACT</b> Unclassified	<b>20. LIMITATION OF ABSTRACT</b> SAR	

PREFACE

The authors wish to express thanks to Harald Weber, a visiting scientist from the German Military Geophysical Office, Trarbach FRG. Mr. Weber played the major role in developing the transformation scheme which allowed him to merge the AFWIND and AFTOX models into a single complex terrain dispersion model, WADOCT.



Approved for Release	
By Special Agent	
Date	
Initials	
Signature	
By	
Date	
Initials	
Signature	
By	
Date	
Initials	
Signature	
A-1	

## Contents

1. INTRODUCTION	1
2. TECHNICAL DISCUSSION	2
2.1 Windflow	2
2.2 Diffusion	5
2.3 The Transformation Scheme	7
3. DIFFUSION TEST DATA	10
3.1 AMADEUS Field Study	10
3.1.1 Program Description	10
3.1.2 Site Location and Description	10
3.1.3 Meteorological Conditions	10
3.1.4 Meteorological Sensors	11
3.1.5 Diffusion	11

3.2 Mountain Iron Field Study	12
3.2.1 Program Description	12
3.2.2 Site Location and Description	13
3.2.3 Meteorological Conditions	13
3.2.4 Meteorological Sensors	13
3.2.5 Diffusion	13
4. MODEL EVALUATION	16
4.1 AMADEUS	16
4.1.1 General	16
4.1.2 Windflow Evaluation	17
4.1.3 Dispersion Evaluation	21
4.2 Mountain Iron	28
4.2.1 General	28
4.2.2 Plume Comparison	31
4.2.3 Statistical Evaluation	31
5. CONCLUSIONS	40
REFERENCES	41

## Illustrations

1. Diagram Showing Grid Structure and Geometry of Model Domain, With Structure of Individual Flux Box.	4
2. Relationship Between the Gaussian Coordinate System and the Wind Flow Coordinate System.	8
3. AMADEUS Terrain Map Showing the Locations of the Meteorological Stations, Samplers, and Release Sites.	11
4. Terrain Map of the Mountain Iron Field Site.	14
5. Source and Sampler Locations for Mountain Iron Diffusion Tests.	15
6. The WADOCT-derived 1000 PPT Concentration Line, and the Measured Concentration Values for the 5-min. Period Surrounding the Indicated Time. Results are for Test Number 6.	23
7. Same as Figure 6 Except for Test Number 7. Underlined Values Represent SF6 Concentrations.	24
8. Same as Figure 7 Except for First Part of Test Number 8.	25
9. Same as Figure 7 Except for Second Part of Test Number 8.	26
10. Same as Figure 7 Except for Test Number 10.	27
11. The 1-hr Mean Actual Plume and Model-derived Plume for Test Number 7. Contours are in PPT.	29

12. Same as Figure 11 Except for Test Number 10	30
13. Actual and Model-Derived Concentration Contour Plots for Test Number 60. Conducted at 1255 PST on 27 Apr 66. Concentration Contours are Normalized Concentrations, $C/Q$ ( $10^9 \text{ sec/m}^3$ ).	32
14. Same as Figure 13 Except for Test Number 81, Conducted at 2040 PST on 2 June 1966.	33
15. Same as Figure 13 Except for Test Number 90, Conducted at 1906 PST on 6 July 1966.	34
16. Scatter Plot of the Observed and Calculated Distances From Source A for Daytime Cases. Dashed lines are the Factor of Two Limits.	36
17. Same as Figure 16 Except for Nighttime.	37
18. Same as Figure 16 Except for Source B.	38
19. Same as Figure 16 Except for Source B and Nighttime.	39

## Tables

1. Date and Time of Available Wind Data from AMADEUS Field program.	12
2. RMSE Statistics for Wind Direction and Wind Speed for Four Cases.	18
3. Deviation of the Mean and Predicted Wind Direction and Speed from the Measured Winds.	19
4. RMSE Statistics for Wind Direction and Wind Speed for Six Stations for Four Cases.	20
5. Tracer Release Data for the Four AMADEUS Tests Used in the Evaluation.	21
6. Percentage Distribution of Calculated vs Observed Distances by Source and Time of Day.	35

# WADOCT—An Atmospheric Dispersion Model for Complex Terrain

## 1. INTRODUCTION

The U. S. Air Force handles, stores and transports a large variety of chemicals in its everyday operation. As a result, atmospheric dispersion models are used as an aid in evaluating potential hazards and developing contingency plans, and are used by emergency response teams as a basis for taking appropriate action in the event of an actual toxic chemical release. Currently, the Air Force uses the dispersion model, AFTOX, for most of its spill scenarios. Although AFTOX allows for varying surface roughnesses, it assumes a spatially uniform windfield throughout the domain. In reality, the windfield may not be uniform in a complex terrain area.

The use of AFTOX is appropriate for most Air Force bases since they are generally located in relatively flat areas. However, some bases, such as Vandenberg AFB, California, may be better served by a complex terrain dispersion model.

This report describes a complex terrain dispersion model called WADOCT (Wind and Diffusion Over Complex Terrain). WADOCT is a microcomputer-based model, capable of running on most IBM compatible machines with enhanced graphics. The program is written in FORTRAN 77, while the graphics module is written in BASIC. WADOCT is user-friendly; the operator is prompted by menu-driven screens. All meteorological and spill data input is manually entered. A terrain input data file, consisting of terrain heights and vegetation heights or surface roughness, is required. Due to limited computer storage capacity, the maximum number of grid points

---

(Received for publication 7 May 1990)

allowed is approximately 5700, or a 75 x 75 array. The most desirable grid spacing is in the range of 100 to 200 m, thus resulting in a maximum areal coverage of 15 x 15 km.

Section 2 of this report is a technical description of the model. Section 3 briefly describes the AMADEUS diffusion experiment conducted in northern California in 1987 and the Mountain Iron diffusion experiments conducted over South Vandenberg AFB, California in 1965 and 1966. Section 4 is an evaluation of WADOCT using some of the data from these two sets of diffusion experiments.

## 2. TECHNICAL DISCUSSION

WADOCT can be divided into three parts: 1) the windflow model, 2) the diffusion model, and 3) the plume/windflow transformation scheme. This section describes these three components of the model. For greater detail on the equations and physics of the windflow model, the reader is referred to Lanicci<sup>1</sup>, Lanicci and Weber<sup>2</sup>, Lanicci and Ward<sup>3</sup>, and Kunkel<sup>4</sup>. For more details on the diffusion model, the reader is referred to Kunkel<sup>5</sup>.

### 2.1 Windflow

The windflow portion of WADOCT produces a two-dimensional (x-y plane) surface-layer windflow analysis using a variational analysis technique employing Gauss's Principle of Least Constraints to induce an initial windfield to conform to constraints of topography, mass conservation, momentum advection, and buoyancy forces. The driving equations for this system attempt to minimize a volume integral relating momentum advection to buoyancy forces. When the minimum value is attained, the system is said to be in a quasi-steady state balance between the constraints. The basic model equation is:

$$\int_{vol} (\vec{A} - \vec{B}) dV = R. \quad (1)$$

---

<sup>1</sup>Lanicci, J.M. (1985) *Sensitivity Tests of a Surface-Layer Windflow Model to Effects of Stability and Vegetation*, AFGL-TR-85-0285, ADA169136.

<sup>2</sup>Lanicci, J.M., and Weber, H. (1986) *Validation of a Surface-Layer Windflow Model Using Climatology and Meteorological Tower Data From Vandenberg AFB, California*, AFGL-TR-86-0210, ADA 178480.

<sup>3</sup>Lanicci, J.M., and Ward, J. (1987) *A Prototype Windflow Modeling System for Tactical Weather Support Operations*, AFGL-TR-87-0159, ADA 189362.

<sup>4</sup>Kunkel, B.A. (1988) *User's Guide for the Air Force Surface-Layer Windflow Model (AFWIND)*, AFGL-TR-88-0157, ADA 208710.

<sup>5</sup>Kunkel, B.A. (1988) *User's Guide for the Air Force Toxic Chemical Dispersion Model (AFTOX)*, AFGL-TR-88-0009, ADA199096.

where the integral is taken over the entire volume of the model domain,  $\vec{A}$  denotes the acceleration represented by the advection terms of the momentum equation,  $\vec{B}$  is the surface parallel component of the buoyancy, and  $R_t$  is the total residual calculated from the integral. The integral is taken over the volume of the model surface layer, which is divided into "flux boxes" of surface normal thickness of 10 m, conforming to the warped terrain surfaces. The coordinate system is used to include effects of terrain slopes in the calculations. The total constraint integral is expressed as a sum over all the boxes in the model layer:

$$R_t = \sum_{i,j} R_{i,j}, \quad (2)$$

where  $R_{i,j}$  is the individual residual at each grid point  $i, j$ .

A number of relaxation sweeps are performed in the model to compute a velocity correction proportional to the steepest descent vector in the multi-dimensional velocity space, written in Eq. (3):

$$n_{i,j}^k = -(\partial R_{i,j} / \partial v_{i,j}^k) / \left[ \sum_{i,j} (\partial R_{i,j} / \partial v_{i,j}^k)^2 \right]^{1/2} \quad (3)$$

where  $k = 1, 2$  and denotes the  $u, v$  wind components,  $n$  is a nondimensional correction factor, and  $v$  is the velocity. The velocity correction is given by the relation:

$$\Delta v_{i,j}^k = 0.03 v_o \sqrt{NM} \cdot n_{i,j}^k, \quad (4)$$

where  $\Delta v_{i,j}^k$  is the velocity correction at  $i, j$ ,  $v_o$  is the initial velocity, and  $N, M$  are the grid dimensions. The relaxation sweeps and windfield adjustments are performed until the first minimum of the residual  $R_{i,j}$  over the domain is achieved.

In the acceleration term  $\vec{A}$ , only the advection  $V \cdot \nabla V$  is a contributing factor. The assumption is made that steady state conditions (that is,  $\gamma V / \gamma t = 0$ ) exist.

The terrain-following coordinate system employed in the model uses a staggered-grid system. Terrain elevations are on one set of grid points, with wind calculation grid points staggered in between, so that calculated terrain slopes can be used in the model integration. The single-layer formulation of the model is represented by using the flux through boxes of thickness  $Z_c$ , whose corners correspond to the terrain grid points. A schematic diagram of these flux-box elements on the model domain is shown in Figure 1. The momentum flux through each face of the flux box is

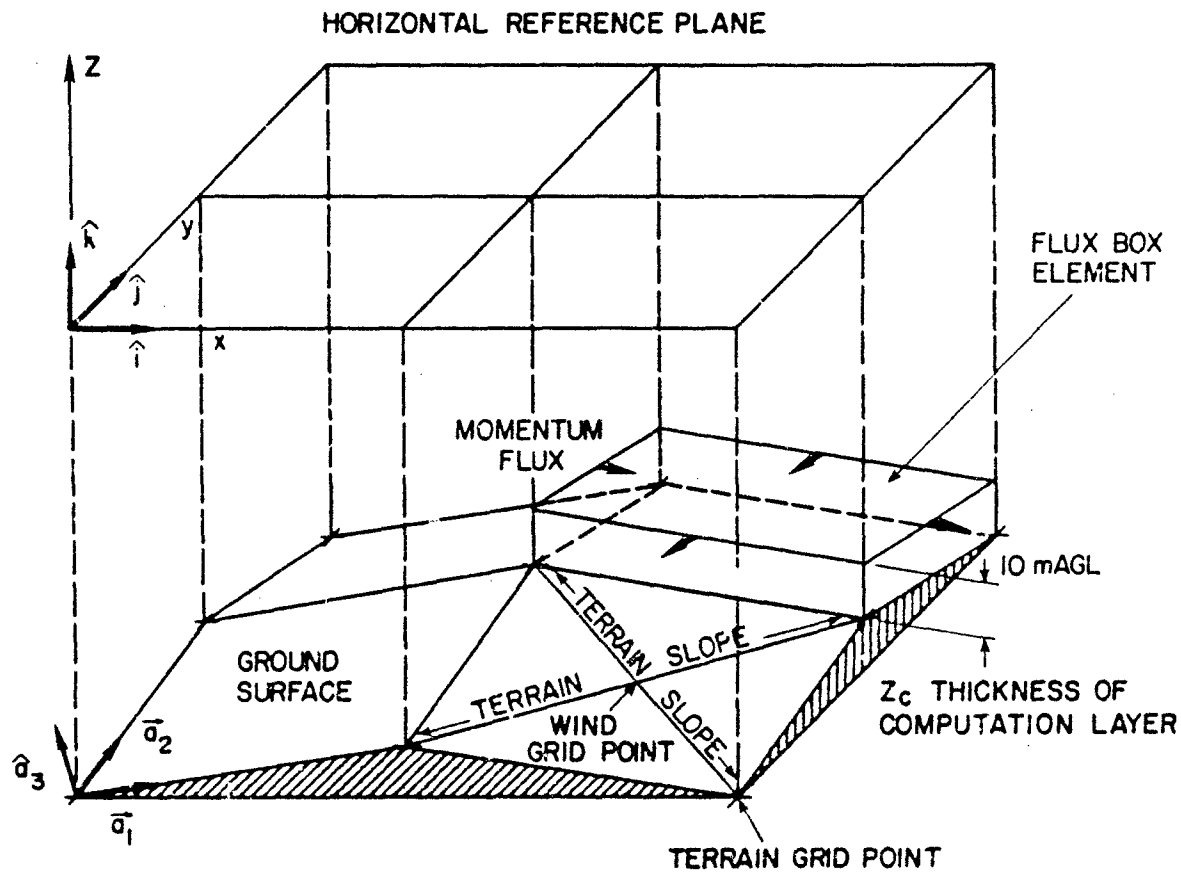


Figure 1. Diagram Showing Grid Structure and Geometry of Model Domain, With Structure of Individual Flux Box.

calculated and modified by the effects of the local surface-layer stability to determine the contribution of each flux-box element to the  $\vec{A}$  term of Eq. (1).

The buoyancy term,  $\vec{B}$ , is a function of the potential temperature gradient as defined in Eq. (5):

$$\vec{B} = \vec{g} \frac{(\theta_o - \theta_s)}{\theta_o} \quad (5)$$

where  $\vec{g}$  is the surface parallel component of the gravitational acceleration,  $\theta_s$  is the surface potential temperature, and  $\theta_o$  is a reference potential temperature above the surface. In the model, the buoyancy,  $\vec{B}$ , is calculated using a form of Eq. (5) modified for use of temperature instead of potential temperature:

$$\bar{B} = \bar{g} \frac{(T_o - T_s + \gamma \Delta Z)}{T_o} \quad (6)$$

where  $T_o$  and  $T_s$  are the upper and lower temperature measurements, respectively,  $\Delta Z$  is the height difference between the two measurements, and  $\gamma$  is the adiabatic lapse rate (1.0°C/100 m).

In the model,  $T_o$  and  $T_s$  are taken either directly from tower or sounding temperature measurements or, if only one temperature measurement is available, derived from the stability computed in the diffusion part of the model. In the latter case, the vertical temperature difference,  $T_o - T_s$ , is related to the stability as given in USNRC Regulatory Guide 1.23<sup>6</sup>, and summarized by Table 1 in Sedeflan and Bennett<sup>7</sup>. This relationship between the stability parameter and the temperature difference can be defined by:

$$T_o - T_s = [0.05 \exp(0.827 SP)] - 2 \quad (7)$$

where the vertical temperature difference is over a 100 m depth. SP is a continuous stability parameter defined in Kunkel<sup>5</sup>. This value varies from 0.5 for very unstable cases to 6.0 for very stable cases. A value of 3.5 is considered neutral.

Temperature gradient data from more than one tower, and also more than one wind measurement can be entered. In the case of a single temperature gradient or temperature measurement and a single wind measurement, the model begins its relaxation steps with a uniform buoyancy and windfield over the domain. When multiple temperature measurements or wind measurements are input, an objective analysis of buoyancy and/or winds is performed to produce nonhomogeneous initial wind and buoyancy fields. The objective analysis procedure is a straightforward technique using a weighting function based on the square of the distance between each of the observation points and the grid points, analogous to the method of Cressman<sup>8</sup>. Once the initial wind and buoyancy fields are established, the model then proceeds with the variational analysis.

## 2.2 Diffusion

The diffusion part of the model is the AFTOX diffusion model, developed by Kunkel<sup>5</sup>. The AFTOX model is a Gaussian puff/plume model designed to handle continuous and instantaneous liquid and gas releases. It contains a library of chemical data for 76 chemicals, but may be run for other chemicals as well.

The Gaussian puff model uses an equation to describe the dispersion of a puff with time. The equation assumes that the material is conserved during transport and diffusion, that is,

<sup>6</sup>USNRC (1972) *Onsite Meteorological Programs Regulatory Guide 1.23*, U.S. Nuclear Regulatory Commission.

<sup>7</sup>Sedeflan, L., and Bennett, E. (1980) A comparison of turbulence classification schemes, *Atmos. Environ.* **14**:741-750.

<sup>8</sup>Cressman, G.P. (1959) An operative objective analysis scheme, *Mon. Wea. Rev.* **87**:367-374.

there is no decay or deposition. It further assumes that the distribution of concentration within the puff is Gaussian.

The Gaussian puff equation can be written

$$G(x, y, z, t - t') = \frac{Q(t')}{(2\pi)^{3/2} \sigma_x \sigma_y \sigma_z} \cdot \exp\left\{-0.5\left[\frac{x - u(t - t')}{\sigma_x}\right]^2\right\} \cdot \exp\left[-0.5\left(\frac{y}{\sigma_y}\right)^2\right] \cdot \left\{\exp\left[-0.5\left(\frac{z - H}{\sigma_z}\right)^2\right] + \exp\left[-0.5\left(\frac{z + H}{\sigma_z}\right)^2\right]\right\} \quad (8)$$

where  $G$  is the concentration in the puff at a given point  $(x, y, z)$  and time  $(t - t')$ .  $Q$  is the total mass in the puff. The diffusion parameters,  $\sigma_x$ ,  $\sigma_y$ ,  $\sigma_z$ , are the standard deviation of the material concentration in the  $x$ ,  $y$ , and  $z$  directions. It is assumed that  $\sigma_x = \sigma_y$ , thus producing a circular horizontal puff cross-section. The variable  $t$  represents the total elapsed time since the spill, and  $t'$  is the time of emission of the puff. Thus,  $(t - t')$  is the travel time or elapsed time since the puff emission.  $u$  is the wind speed at 10 m and  $H$  is the height of the source. If there is an inversion whose base is above the ground, then additional terms are added to Eq. (8), (see Kunkel<sup>5</sup>).

The concentration at a point in space at a given time depends on the number of nearby puffs, their size, and the amount of material in each puff. The sum effect of all these puffs is given by summing over all emission times:

$$C(x, y, z, t) = \sum_{t=0}^{\infty} G(x, y, z, t - t') \quad (9)$$

For a continuous spill, or a spill of finite duration, the summation is performed over puffs whose centers are located within four standard deviations of the puff concentrations upwind and downwind from the location of interest. It is assumed that concentrations from puffs further than four standard deviations contribute little to the concentration at the specified location.

For an instantaneous gas release there is only one emission time and one puff. Therefore, a summation is not necessary. The number of puffs for a continuous release varies from 4 to 20 puffs per minute depending on the distance from the source and the wind speed.

The dispersion parameters ( $\sigma_x$ ,  $\sigma_y$ ,  $\sigma_z$ ) are a function of the atmospheric stability and distance from the source. In diffusion modeling, the atmospheric stability is often defined by the Pasquill stability categories which range from a category of A (for a very unstable atmosphere) to F (for a very stable atmosphere). In this model, a continuous stability parameter ranging from 0.5 to 6 is used in place of the discrete stability categories. This prevents sharp changes in the hazard distance when going from one stability category to another; this can happen with a slight change in wind speed, solar angle or cloud cover.

The diffusion model uses one of two methods to determine the stability parameter: (1) relates the wind speed and solar insolation to a stability parameter, or (2) uses the standard deviation of

the horizontal wind direction to define the stability parameter. In the first method, the Monin-Obukhov length is computed from the wind and solar input data and, along with the surface roughness, is then related to a stability category through a method described by Golder<sup>9</sup>. In the second method, the stability is determined using the Modified Sigma Theta (MST) approach described by Mitchell<sup>10</sup>.

The Pasquill-Gifford dispersion parameters are used in the dispersion model. These values are based on a surface roughness of 3 cm and a concentration averaging time of 10 min. The model adjusts the dispersion parameters for other surface roughnesses and concentration averaging times.

The model contains two evaporation models that are used for calculating the source strength from evaporating pools. Most of the liquid chemicals in the chemical data file use the Shell evaporation model (Fleischer<sup>11</sup>) which computes the mass transfer from the pool to the atmosphere due to forced convection over the liquid pool due to the wind. The model assumes that mass evaporated by heat transfer is negligible. The model requires such data as critical pressure, temperature and volume, vapor pressure, liquid density, and molecular diffusivity. If only the vapor pressure is known, the Clewell evaporation model<sup>12</sup> is used. The Clewell model is a crude approximation to the Ille and Springer evaporation model<sup>13</sup>. For more details on these models the reader can refer to the cited references or to Kunkel<sup>14</sup>.

### 2.3 The Transformation Scheme

Once the wind field has been determined and the concentration contours, based on a horizontally homogeneous wind field have been calculated, points along the contours are repositioned as we convert from a Gaussian coordinate system to a windflow coordinate system. In the Gaussian coordinate system, the origin is at the spill source and the x-axis is along the downwind direction. In the windflow coordinate system, the origin is located in the lower left-hand corner of the specified domain, and the x-axis is in the west-east direction. The problem, as illustrated in Figure 2, is to take point P with coordinates Gx and Gy in the Gaussian coordinate system, and locate it in the windflow coordinate system.

---

<sup>9</sup>Golder, D. (1972) Relations between stability parameters in the surface layer, *Boundary Layer Met.* **3**:46-58.

<sup>10</sup>Mitchell, A.E., Jr. (1982) A comparison of short-term dispersion estimates resulting from various atmospheric stability classification methods, *Atmos. Environ.* **16**:765-773.

<sup>11</sup>Fleischer, M.T. (1980) *SPILLS—An Evaporation/Air Dispersion Model for Chemical Spills on Land*, Shell Development Company, PB 83109470.

<sup>12</sup>Clewell, H.J. (1983) *A Simple Formula for Estimating Source Strengths from Spills of Toxic Liquids*, ESL-TR-83-03.

<sup>13</sup>Ille, G., and Springer, C. (1978) *The Evaporation and Dispersion of Hydrazine Propellants from Ground Spills*, CEEDO-TR-78-30.

<sup>14</sup>Kunkel, B.A. (1983) *A Comparison of Evaporative Source Strength Models for Toxic Chemical Spills*, AFGL-TR-83-0307, ADA139431.

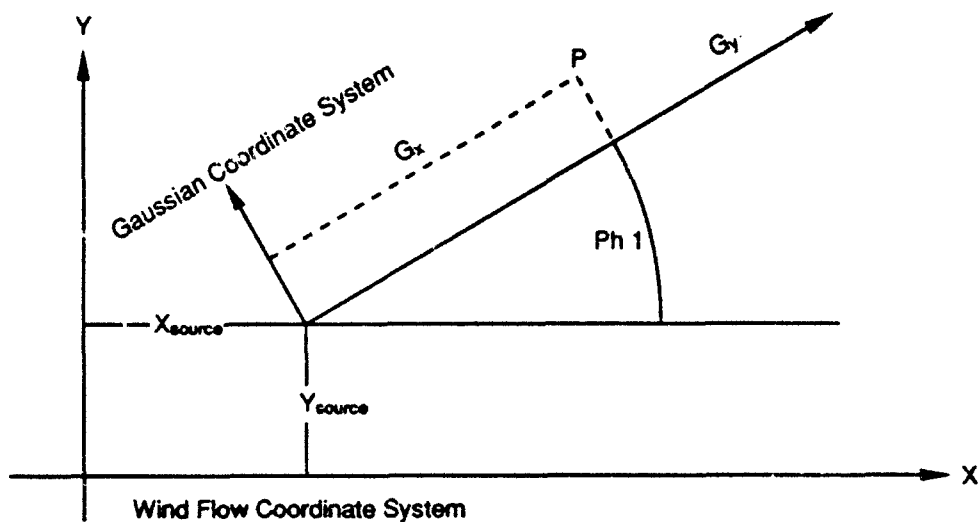


Figure 2. Relationship Between the Gaussian Coordinate System and the Wind Flow Coordinate System.

The concentration at P is a result of the transport of the released chemical by the mean wind and by diffusion processes. The first step in switching coordinate systems is to calculate the travel time,  $t$ , from the source to P using the mean wind in the Gaussian system,  $U$ :

$$t = Gx/U \quad (10)$$

where  $U = (u^2 + v^2)^{1/2}$ , and  $u$ ,  $v$  are the components of the mean wind in the wind flow coordinate system.

The next step is to divide this time into small time steps,  $Dt$ . The time steps should be chosen so that  $Dt$  is less than  $Dx/U$ , where  $Dx$  is the grid width of the windflow model used to provide the wind data input.

For a given  $Dt$ , the number of necessary time steps can be determined.

$$N = \text{INT} (t/Dt) \quad (11)$$

where INT is the integer function.

Using  $N Dt$  as travel time, we can calculate the diffusion velocities for the particles.

$$UdG = Gx/(N Dt) \quad (12a)$$

$$VdG = Gy/(N Dt) \quad (12b)$$

These Gaussian wind velocity components have to be transformed into the coordinate system used for the windflow model using the following equations:

$$U_d = U_dG \cos(\Phi_i) - V_dG \sin(\Phi_i) \quad (13a)$$

$$V_d = U_dG \sin(\Phi_i) + V_dG \cos(\Phi_i) \quad (13b)$$

where  $\Phi_i$  is the angle between the mean wind and the x-axis of the windflow coordinate system. The wind field can be divided into the mean and the perturbation field:

$$u = \bar{u} + u' \quad (14a)$$

$$v = \bar{v} + v' \quad (14b)$$

Starting at the source, the particles are transported for N time steps using the diffusion velocity components plus the perturbation components of the wind field as the transporting velocities:

$$\begin{aligned} \text{for } i = 1: \quad & x(i) = x_{\text{source}} \\ & y(i) = y_{\text{source}} \end{aligned} \quad (15)$$

$$\begin{aligned} \text{for } i > 1: \quad & x(i) = x(i-1) + \Delta t \{u'[x(i-1), y(i-1)] + U_d\} \\ & y(i) = y(i-1) + \Delta t \{v'[x(i-1), y(i-1)] + V_d\} \end{aligned}$$

with  $u'[x(i-1), y(i-1)]$  and  $v'[x(i-1), y(i-1)]$  as weighted average values calculated from the grid values:

$$\text{for } i = N: \quad x(N), y(N) = \text{new coordinates in the inhomogeneous wind field for point P in the Gaussian coordinate system.}$$

The concentration at P in the Gaussian coordinate system is then transferred to point  $x(N), y(N)$  in the windflow coordinate system.

This procedure can be used to transform any coordinate point from the Gaussian system to another coordinate system using any wind field. If a homogeneous wind field is used for the transformation, the Gaussian contour lines will not be changed.

### 3. DIFFUSION TEST DATA

Data from two different field experiments were used to evaluate the WADOCT model. These experiments were the AMADEUS experiments<sup>15</sup> conducted in Northern California in 1987, and the Mountain Iron experiments<sup>16,17</sup> conducted at Vandenberg AFB, California in 1965 and 1966.

#### 3.1 AMADEUS Field Study

##### 3.1.1 PROGRAM DESCRIPTION

The objective of the AMADEUS program was to collect a comprehensive meteorological and diffusion data base for the test and evaluation of complex terrain transport and diffusion models. The program was conceived and managed by the U. S. Army Atmospheric Sciences Laboratory, but other Army laboratories and the Air Force Geophysics Laboratory participated in and supported the program. AMADEUS was conducted during the fall phase of Project WIND from 23 September through 3 October 1987.

##### 3.1.2 SITE LOCATION AND DESCRIPTION

The field site known as Meadowbrook (situated in the foothills on the west side of the Sierra Nevada Mountain range), is located 15 miles northeast of Red Bluff, CA. The Meadowbrook area consists of a broad flat valley oriented east-west along Paynes Creek. The west end of the valley opens up into a broad, relatively flat area, while the east end is characterized by a V-shaped ridge extending into the valley separating Paynes and Plum Creeks. The valley floor is grass-covered, while the side walls and the adjacent plateau have some shrubs and sparse trees. The terrain contours (in 10-meter increments) are shown in Figure 3. Elevations range from 365 m above sea level in the valley to a maximum elevation of 550 m along the east edge. The height of the valley wall is approximately 60 m.

##### 3.1.3 METEOROLOGICAL CONDITIONS

One of the primary reasons for choosing this site was the very predictable occurrence of two well-defined flow regimes. One was the daytime westerly upslope flow (unstable) from about 0900 to 1700 hours (PDT), and the other was the easterly downslope (stable) drainage winds from about 1900 to 0600. During this time of year, the area is characterized by moderate-to-strong synoptic scale subsidence.

---

<sup>15</sup>Cionco, R.M. (1989) *AMADEUS: A Dispersion Study Over Moderately Complex Terrain*, Preprint Volume of the 6th Joint Conference on Applications of Air Pollution Meteorology, Anaheim, Calif.

<sup>16</sup>Hinds, W.T., and Nickola, P.W. (1967) *The Mountain Iron Diffusion Program: Phase I South Vandenberg: Volume I*, AFWTR-TR-67-1, AD 721858.

<sup>17</sup>Hinds, W.T., and Nickola, P.W. (1968) *The Mountain Iron Diffusion Program: Phase I South Vandenberg: Volume II*, AFWTR-TR-67-1, AD 721859.

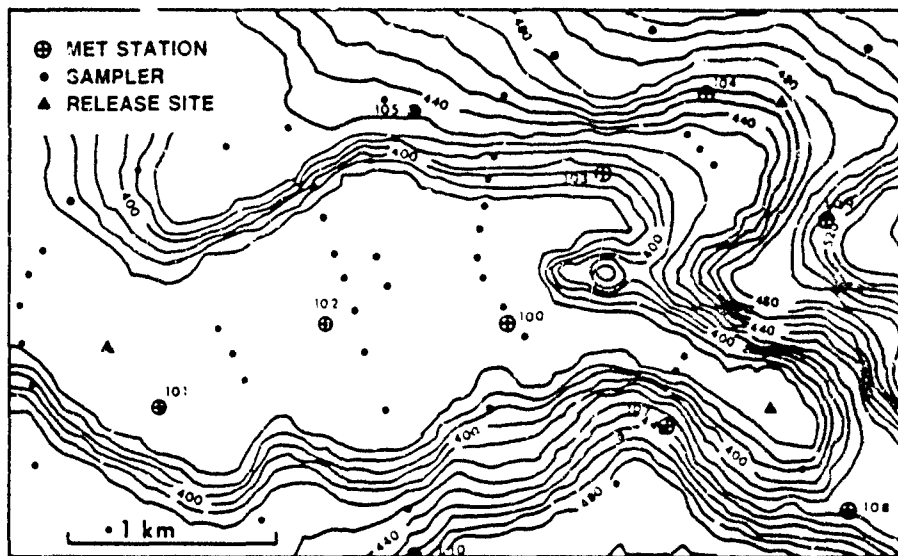


Figure 3. AMADEUS Terrain Map Showing the Locations of the Meteorological Stations, Samplers, and Release Sites.

#### 3.1.4 METEOROLOGICAL SENSORS

There was a large array of meteorological sensors positioned throughout the area. Ten meteorological stations were used in this evaluation of WADOCT; their positions are shown in Figure 3. Each station measured wind speed and wind direction at 10 m, and temperature at 2 m and 10 m. Other instrumentation available, but not used in this study, included a 32-m mast with wind and temperature measurements at 2, 4, 8, 16, and 32 meters, two three-dimensional sonic anemometer-thermometer units, and a doppler sodar for measuring the three-dimensional winds in the first 150 m of the boundary layer. Three sets of laser anemometers were installed at three levels across the valley to establish the cross-sectional bulk flow along the valley axis. Upper air soundings were also obtained prior to each diffusion experiment.

#### 3.1.5 DIFFUSION

For the diffusion experiments, two inert and invisible gas tracers were released at different heights, time periods, and locations for both stable and unstable atmospheric conditions. The gas tracers were sulphur hexafluoride ( $\text{SF}_6$ ) and bromotrifluoromethane (B3FM). During daytime experiments, the tracer release site was located at the west end of the valley. During nighttime experiments, the tracer was released from the Paynes Creek and/or the Plum Creek Canyon. Some 50 sampler sites were located in rows normal to the valley, the Plum Creek and Paynes Creek Canyons and along the top of the side walls of the valley. Each site had 24 bag samplers programmed to intake 5-min samples sequentially to cover the two-hour trial period. The tracer samples were analyzed off site with gas chromatography technology. The location of the release sites and sampler sites are shown in Figure 3.

Smoke tests were often conducted at the same time as the gas tracer releases to obtain a visual picture of the flow patterns. Some quantitative data was obtained with bubblers and photometers, and visual documentation of the plume behavior was obtained by means of ground-level (lateral view) and aerial photography, and video tape recording.

A total of ten tests plus a trial run (number 1) were conducted during the 2-week program. The tests were evenly divided between unstable and stable conditions. All tracer releases occurred over a 2-hr period except for two tests (number 8, number 9) which consisted of two 15-min releases with a 1-hr separation time.

The wind data that were used for evaluating WADOCT were taken over a 4-hr period around each test. These time periods are listed in Table 1. The tracer releases started 1 hr after the start of the wind measurements. Also shown is whether it was an upslope (unstable) or downslope (stable) case.

Table 1. Date and time of available wind data from AMADEUS field program.

TEST #	DATE	TIME	CONDITION
1	21 Sep 87	1204-1604	upslope
2	23 Sep 87	1300-1700	upslope
3	24 Sep 87	2244-0244	downslope
4	26 Sep 87	1100-1500	upslope
5	27 Sep 87	0218-0618	downslope
6	28 Sep 87	0938-1338	upslope
7	29 Sep 87	2000-0000	downslope
8	30 Sep 87	1825-2225	downslope
9	1 Oct 87	1200-1600	upslope
10	2 Oct 87	1117-1517	upslope
11	3 Oct 87	1817-2217	downslope

### 3.2 Mountain Iron Field Study

#### 3.2.1 PROGRAM DESCRIPTION

The objective of the Mountain Iron diffusion program was to collect a comprehensive meteorological and diffusion data base in order to develop an empirical diffusion model specifically for South Vandenberg. A total of 102 successful tests were conducted during an 8-mo period from December 1965 through July 1966. The tests were sponsored by the Air Force and conducted by the Pacific Northwest Laboratory of the Battelle Memorial Institute of Richland, Washington.

### 3.2.2 SITE LOCATION AND DESCRIPTION

South Vandenberg is bordered on the west and south by the Pacific Ocean. Figure 4 is a topographic map of South Vandenberg showing the irregular and rugged terrain with a number of canyons, ridges and peaks. The most prominent features identified on the map are the rather deep and steep-sided Honda Canyon with Target Ridge on the north side and Honda Ridge on the south side. The canyon, oriented east-west, is some 200-300 m deep along most of its length, and is generally no more than 3 km across. Many smaller canyons branch from these two main ridges. During the field experiments tracer releases were made from two sources. They were Source A, the primary source, at VIP-1 and Source B at Area 529 shown in Figure 5.

The vegetation varies from grasslands in the lower, flatter areas to dense stands of low-growing shrubs along the ridges. Trees occur in scattered clumps throughout the area.

### 3.2.3 METEOROLOGICAL CONDITIONS

Wind directions are predominantly from the northwest quadrant, decreasing somewhat at night, but then increasing during the day. There is almost always a maritime inversion whose base is several hundred meters above sea level. However, quite often the inversion base is below the higher terrain. It is not apparent as to whether this actually occurred during any of the tests.

### 3.2.4 METEOROLOGICAL SENSORS

The number and types of meteorological instrumentation varied during the 8-month field program. About 15 wind sensors were located throughout the area, including at the source. Vertical temperature gradients were obtained from temperature sensors mounted at various levels of 18- and 92-m towers. Wiresonde and radiosonde data were also collected at various times.

### 3.2.5 DIFFUSION

The tracer material used during these experiments was the fluorescent pigment, zinc sulfide. It is a very fine particulate that fluoresces green under ultraviolet light. This is the same tracer used in other diffusion experiments such as Ocean Breeze, Dirty Gulch, and Green Glow.

The sampler used in the tests was a membrane filter inserted in a disposable polyethylene holder. Samples collected on the filter were bulk samples intended to collect all pigment passing through the intake during a given run. As was stated by Hinds and Nickola<sup>16</sup>, diffusion tests are usually designed with sampling arcs concentric about the release point and spaced logarithmically to account for the expected power-law decrease of exposure with distance. Due to the irregular terrain of South Vandenberg, the sampling grid was laid out along irregular lines with respect to the source points. Existing roads and jeep trails were used as sampling routes as shown in Figure 5. Confining the sampling to existing roads posed a number of problems. One consequence of the sampling grid arrangement was to provide poor crosswind plume definition for releases from the two sources under certain wind directions. Some of the releases may not have been sampled adequately when the plume axis was aligned with, instead of crossing the sampling route.

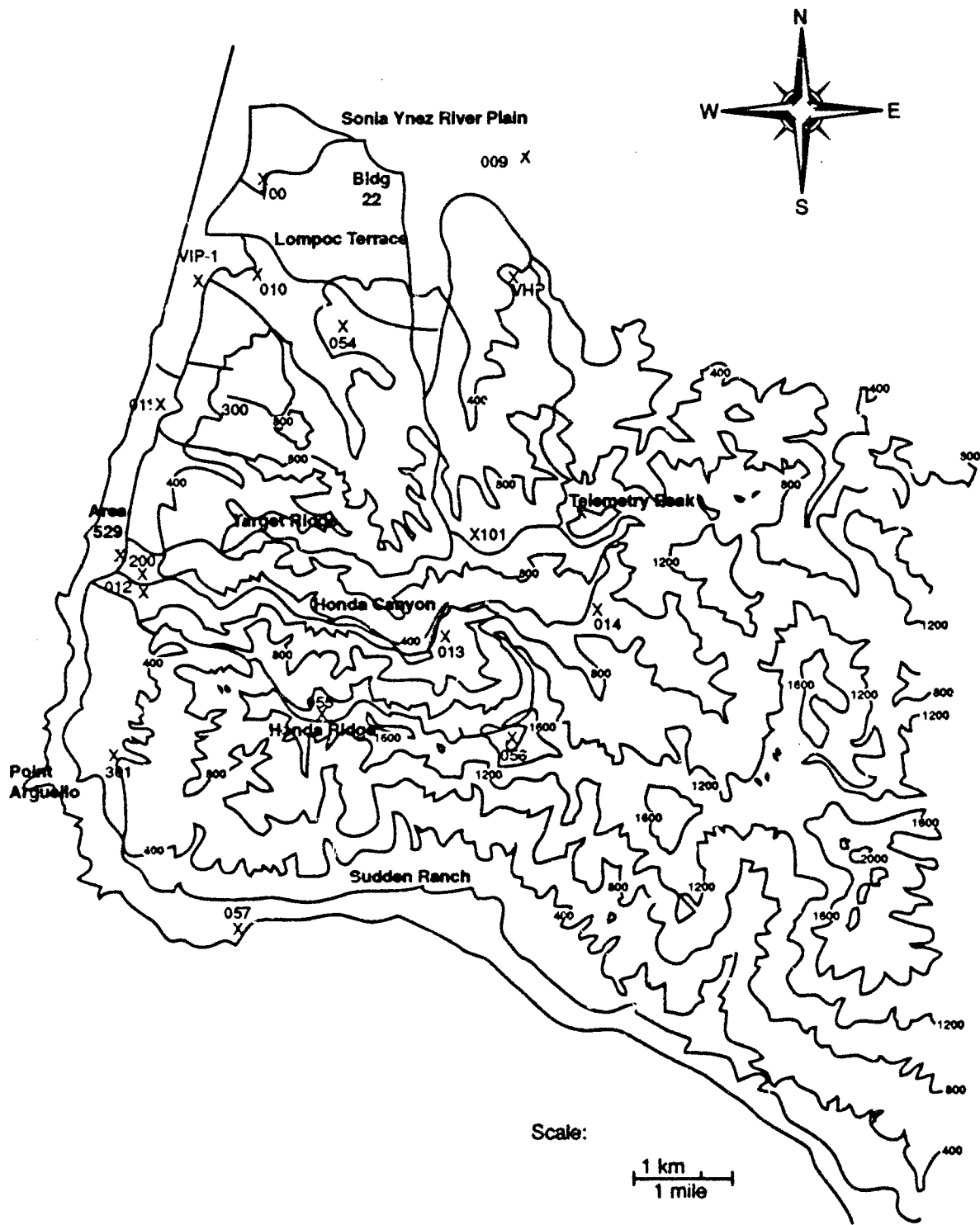


Figure 4. Terrain Map of the Mountain Iron Field Site.



A serious problem encountered during the field experiments was sampler access. During the rainy season, some portions of roads and trails were subjected to washing and flooding, especially in Honda Canyon. Hinds and Nickola remarked that the Honda Canyon sampling route was usable in its entirety for only ten days between late November and March. They also remarked that the available data showed that Honda Canyon caused anomalous diffusion, but that they could not draw any conclusion since a substantial fraction of the test data was unavailable because of inaccessibility.

According to Hinds and Nickola, out of a total of 113 tracer releases from Sources A and B, 102 tests were deemed to be successful. The majority of the releases with a constant and continuous release rate were of 15- or 30-min duration, while nine tests were with duration of only 5 min. Since the test results of these short-term releases differed from the other longer-term releases, the 5-min tests were not considered in this study. Furthermore, due to the absence of the essential wind data at or near the release points, a number of tests were excluded, and the number of test results used in this study was reduced to 87.

#### **4. MODEL EVALUATION**

##### **4.1 AMADEUS**

###### **4.1.1 GENERAL**

With the large array of meteorological data available at the AMADEUS site, there exists a variety of options for wind and temperature input data into WADOCT. Either a single surface temperature, or single- or multiple-temperature profile data can be entered. If a single-surface temperature is input, then the stability, and thus buoyancy, is computed using the mean wind speed and the solar conditions. The actual temperature is not critical to the buoyancy calculation, and, therefore, it makes little difference whether a temperature from a single location or a mean temperature from several locations is used. Buoyancy, however, is very sensitive to the vertical temperature gradient, and therefore, the choice of which temperature profile measurement to use becomes important.

Ten meteorological sites were used in the evaluation using the following input data:

- 1) Mean surface temperature
- 2) Mean temperature difference between 2 and 10 m
- 3) Mean temperature difference between lowest and highest point  
(Tower 109 10-m level — Tower 102 2-m level, a height difference of 142 m)
- 4) Mean wind direction and speed at the 10-m level.

The meteorological data were sampled at a 1-second rate and 1-minute averaged values were recorded.

The model contained a  $44 \times 27$  array which covered the area shown in Figure 3. The grid spacing was 100 m. Both terrain and vegetation heights were included in the array.

The WADOCT model evaluation, using the AMADEUS data, is divided into two parts: 1) an evaluation of just the windflow part of the model, and 2) an evaluation of the dispersion model as a whole.

#### 4.1.2 WINDFLOW EVALUATION

To evaluate the windflow part of the model, the three types of temperature data, cited above, were used for the buoyancy calculations. Two types of wind information were used as input: 1) a single-mean wind from the 10 sites, and 2) the mean winds from each of 4 sites. Ten-minute mean winds were used. Using the single-mean wind as input, the model-predicted winds could be evaluated against the actual winds measured at each of the 10 sites. When four winds were used, the evaluation was carried out at the other six sites. Four sites were picked whose winds appeared to be least affected by the terrain. These sites were 102, 105, 109, and 110.

When a single-mean wind direction and speed are used, the model calculations begin with a uniform wind field over the domain. When more than one wind measurement is used for input, the model initializes the wind field over the domain using an objective analysis scheme.

Of the 10 test periods, it was decided to concentrate on two stable cases (number 7 and number 8) and two unstable cases (number 4 and number 10). Other tests could have been included in the study, but the consistent results obtained from these four test periods lead us to believe that no different conclusions would be drawn by running the model against the other cases. Not all of the tests, including the four chosen for this study, had complete data sets. In Test 7, meteorological station number 109 was not operating and therefore, only three of the four stations were used for input. In Test 8, there were only two hours in which data were obtained from all 10 towers. In Test 10, there were three hours of good data.

To evaluate the effectiveness of the model in adjusting the wind flow to the terrain, RMSE calculations of the actual vs predicted wind speed and wind direction were done for each of the 10 sites when using the mean wind as input, and for the 6 sites when using the winds from the other 4 sites as input. When multiple wind inputs were used, the RMSEs of the initialized, interpolated wind field were calculated. This provided a means of comparing the variational analysis scheme with the simpler objective analysis scheme.

Table 2 shows the wind direction and wind speed RMSE statistics for the 10 met sites and for each of the four cases. The RMSEs are for 10-minute averaged winds starting at the indicated time. The mean wind direction and wind speed for the 10 sites were used for input. The first column of RMSEs in each box is the RMSEs of the mean vs actual wind. Columns 2, 3, and 4 represent the RMSEs using the surface temperature, the mean DT between 2 and 10 m, and the DT between the highest and lowest point, respectively.

For the four cases and for all the time periods, the wind direction RMSEs derived from the model runs are smaller than the RMSEs derived from the mean winds. In other words, wind directions calculated by the model provide a better estimate of the actual wind directions than simply using the mean wind direction. There is no significant difference in the results between the three temperature input conditions. There is also no apparent difference between the stable and unstable cases.

The reverse is true for wind speed. The wind speed statistics show, almost without exception, that the model calculations of the wind speed produce greater deviations from the actual winds than when using the mean wind speed. In fact, there appears to be an inverse correlation between the RMSEs of the wind directions and wind speeds. In other words, the more accurately the wind directions are predicted, the less accurately the wind speeds are predicted. Another interesting observation, not shown in Table 2, is that, in general, the temperature input data that

Table 2. RMSE Statistics for Wind Direction and Wind Speed for Four Cases.  
 Mean Wind Direction and Speed From All Ten Stations Were Used as Model Input.

WIND DIRECTION RMSE (deg)																				
TEST 4				TEST 7				TEST 8				TEST 10								
TIME	WD	TS	DT8	DT142	TIME	WD	TS	DT8	DT142	TIME	WD	TS	DT8	DT142	TIME	WD	TS	DT8	DT142	
1100	30.8	26.5	25.3	25.1	2000	30.0	22.6	26.0	22.6	1930	37.6	31.3	32.2	31.3	1130	32.5	26.3	26.3	26.3	26.3
1130	30.1	23.8	22.4	23.2	2030	28.4	24.4	23.9	20.8	2000	31.9	18.2	25.4	17.5	1200	37.3	30.1	30.1	30.1	30.1
1200	24.8	20.9	18.5	20.8	2100	32.8	30.9	29.0	25.5	2030	31.3	22.4	26.7	21.0	1730	27.8	22.8	22.8	22.8	22.8
1230	26.5	23.1	22.8	22.2	2130	35.4	33.1	31.6	28.7	2100	28.9	24.0	25.6	23.8	1300	27.2	20.4	20.4	20.4	20.4
1300	24.7	21.6	19.0	20.2	2200	34.2	32.4	30.3	27.3						1330	31.7	28.7	28.7	28.7	28.7
1330	33.9	30.5	28.2	28.9	2230	33.8	22.9	28.5	22.2						1400	26.5	22.0	22.0	22.0	22.2
1400	31.3	28.0	25.1	30.7	2300	29.6	13.0	17.1	12.8											
					2330	28.5	18.3	19.9	21.1											
MEAN	28.9	24.9	23.0	24.5		31.6	25.0	25.8	22.6		32.4	24.0	27.5	23.4		30.5	25.0	25.1	25.1	25.1
WIND SPEED RMSE (m/s)																				
TIME	WS	TS	DT8	DT142	TIME	WS	TS	DT8	DT142	TIME	WS	TS	DT8	DT142	TIME	WS	TS	DT8	DT142	
1100	0.54	0.79	0.83	0.83	2000	0.98	0.96	0.89	0.96	1930	0.81	1.12	0.89	1.12	1130	0.29	0.44	0.44	0.44	0.44
1130	0.57	0.86	0.92	0.90	2030	1.13	1.09	1.01	1.17	2000	0.74	1.01	0.75	1.06	1200	0.42	0.59	0.59	0.59	0.59
1200	0.59	0.90	1.04	1.04	2100	0.98	1.03	0.92	0.99	2030	0.68	0.81	0.66	0.89	1230	0.56	0.68	0.68	0.68	0.68
1230	0.83	1.10	1.10	1.10	2130	0.78	0.77	0.67	0.71	2100	0.87	0.91	0.81	0.95	1300	0.48	0.57	0.57	0.57	0.57
1300	0.80	1.10	1.20	1.16	2200	0.70	0.72	0.60	0.69					1330	0.31	0.37	0.37	0.37	0.37	
1330	0.48	0.74	0.81	0.79	2230	0.82	0.95	0.82	0.88					1400	0.59	0.80	0.80	0.77	0.77	
1400	0.87	1.11	1.19	1.11	2300	0.55	0.69	0.59	0.69											
					2330	0.59	0.75	0.64	0.86											
MEAN	0.67	0.94	1.01	0.99		0.82	0.87	0.76	0.86		0.77	0.96	0.78	1.00		0.44	0.57	0.57	0.57	

produced either the greatest stability or instability, produced the smallest wind direction RMSEs and the largest wind speed RMSEs. In other words, adjusting the stability, or buoyancy, does not produce an overall improvement in the model results.

The wind deviations at each met site were checked to insure that no single site was seriously affecting the RMSE statistics. Table 3 shows the mean deviation of the actual wind from the mean wind and from the model predicted wind for each of the ten sites and for the four cases. The table shows that 60 percent of the time the model produces smaller deviations in wind direction than the mean wind direction. For wind speed, however, the model produces smaller deviations than the mean only 28 percent of the time. There do not appear to be any anomalies among the different sites. The greatest wind direction deviations occur at the stations located in the two canyons, namely Sites 103, 104, and 107, where the flow tends to be parallel to the canyon floor. In all cases, the model adjusted the wind direction toward the actual wind directions, but never to the actual wind directions.

Table 3. Deviation of the Mean and Predicted Wind Direction and Speed From the Measured Winds. (Mean or Predicted Wind — Measured Wind)

DEVIATION FROM MEASURED WIND DIRECTION (deg)								
MET SITE	TEST 4		TEST 7		TEST 8		TEST 10	
	MEAN	PREDICTED	MEAN	PREDICTED	MEAN	PREDICTED	MEAN	PREDICTED
101	-12	-11	-13	-11	7	10	-23	-9
102	-13	-13	13	13	8	10	16	8
103	51	39	30	12	26	2	31	5
104	51	46	50	32	49	25	43	26
105	-23	-24	-22	-32	-16	-29	-6	-12
106	-3	-3	17	15	30	31	3	8
107	-24	-10	-55	-35	-56	-24	-31	-7
108	10	17	-13	-8	-17	-8	-17	-8
109	-11	-9			-7	1	10	21
110	-23	-18	-8	-2	-21	-13	-50	-40
MEAN	22	19	25	18	24	15	21	18

DEVIATION FROM MEASURED WIND SPEED (m/s)								
MET SITE	TEST 4		TEST 7		TEST 8		TEST 10	
	MEAN	PREDICTED	MEAN	PREDICTED	MEAN	PREDICTED	MEAN	PREDICTED
101	-1.0	-1.4	1.1	0.8	-0.6	-0.9	0.0	-0.4
102	-0.1	-1.0	0.4	-0.3	-1.0	-1.1	-0.3	-0.4
103	-0.2	-0.4	0.1	0.3	-0.1	-0.4	-0.5	-0.4
104	1.1	0.8	-0.6	-0.8	0.7	0.7	-0.5	-0.7
105	-0.6	-1.7	-0.2	-0.3	0.4	0.2	0.3	-0.1
106	0.1	0.3	-1.4	-1.6	1.3	1.2	0.1	-0.2
107	0.6	0.9	-0.3	-0.1	-0.5	0.0	0.3	0.1
108	-0.4	-0.4	-0.2	0.2	0.1	0.0	0.2	0.2
109	0.8	1.1			-0.1	-1.5	0.2	0.9
110	-0.1	0.1	0.2	0.3	0.0	-1.0	0.3	0.7
MEAN	0.50	0.81	0.45	0.47	0.48	0.70	0.27	0.41



Table 4 shows the wind direction and wind speed RMSE statistics for 6 of the 10 sites and for each of the four cases. The wind direction and speeds from the other four sites were used for input. The first column of RMSEs represents the RMSE of the mean winds from the four sites vs the actual winds from the other six sites. The second column contains the RMSEs from the interpolated winds. Columns 3 and 4 lists the RMSEs of the predicted vs actual winds when using the surface temperature and the mean DT over a 142 m depth, respectively, as input.

The numbers show that the wind field derived from the objective analysis scheme can produce a poorer estimate of the actual wind field than simply assuming a uniform wind field equal to the mean wind of the four input sites. The objective analysis scheme produces higher wind direction RMSEs 60 percent of the time and higher wind speed RMSEs 72 percent of the time. This agrees with the conclusion from the Vandenberg study that the model performs better when the mean vector wind is put in and an objective analysis not performed than when the individual winds are input and an objective analysis is performed.

The overall results are similar to the results when using the mean wind data from all ten stations. As one might expect, the RMSEs are, in general, slightly higher when using meteorological data from four sites than when using data from all ten locations. As in the ten-station analysis, there is no significant difference in the RMSEs between the two temperature input conditions. Again, the model does a poor job of adjusting the wind speeds.

#### 4.1.3 DISPERSION EVALUATION

Initially, the same four tests were evaluated for dispersion patterns, but it was soon realized that in Test 4 the model predicted the plume to go off to the southeast and out of the area covered by the samplers. This trajectory was confirmed by the lack of tracer material detected by the samplers. Consequently, Test 6 was substituted for Test 4. Table 5 shows the release information for the four tests.

Table 5. Tracer Release Data for the Four AMADEUS Tests Used in the Evaluation.

TEST	DATE	TIME (LST)	SF6 RELEASE			B3FM RELEASE		
			RATE (g/s)	HT (m)	LOCATION	RATE (g/s)	HT (m)	LOCATION
6	28 SEP 87	1038-1238	2.54	10	Meadow West	No Release		
7	29 SEP 87	2100-2300	2.74	1	Paynes Creek	5.75	1	Plum Creek
8	30 SEP 87	1925-1940 2040-2055	3.53 3.78	1	Paynes Creek	6.43 6.80	1	Plum Creek
10	2 OCT 87	1217-1417	2.27	10	Meadow West	5.65	10	32 M Tower

Three of the four tests (6, 7, 10) were 2-hr continuous releases. Test 8 consisted of two 15-min releases spaced 1 hr apart. Except for Test 6, the tests consisted of the release of both sulfur hexafluoride and bromotrifluoromethane at different locations as indicated in Table 5.

In running the model to evaluate the dispersion of the tracer, the winds from each of the 10 meteorological sites and an average surface temperature were input. Five-minute sampler data were collected over a 2-hr period, resulting in 24 samples per sampler.

The dispersion pattern was evaluated at 17.5, 27.5 and 52.5 min after the start of the release. These times represent the midpoint of a 5-min sampling period. The short sampling periods resulted in highly variable concentration measurements in both time and space. Consequently, it was very difficult to draw concentration isopleths that could be compared with the model isopleths. One of the contributing factors to the variability may be the fact that the samplers were placed very close to the ground surface, and in many cases the plumes may have gone over the sampler, especially during the daytime cases. At night, the model indicates that the plume could have been narrow enough to pass between samplers or passed over, at most, one sampler along a row.

Figures 6 through 10 show the 1000 PPT concentration line for different times after the start of release as computed by the model. Also shown are the measured concentrations for the 5-min period surrounding the indicated time. The underline values are for the tracer SF<sub>6</sub>. It should be pointed out that the threshold value for SF<sub>6</sub> is 500 PPT and for B3FM is 100 PPT. It is, therefore, quite possible that minute quantities of tracer were present, but not detected by the samplers.

For two of the cases (Tests 7 and 10), the sampler data were averaged over a 1-hr period to obtain a better representation of the mean plume. Test 6 was excluded because there was not sufficient sampler data over a 1-hr period to produce a Gaussian type plume. Test 8 was excluded because it consisted of two 15-min releases. The mean concentrations for a one-hour period, derived from the twelve 5-min samples, are undoubtedly very conservative values since the measured concentrations for many of the 5-min periods were below the sampler threshold, and thus, not included in the calculation of the overall mean concentration.

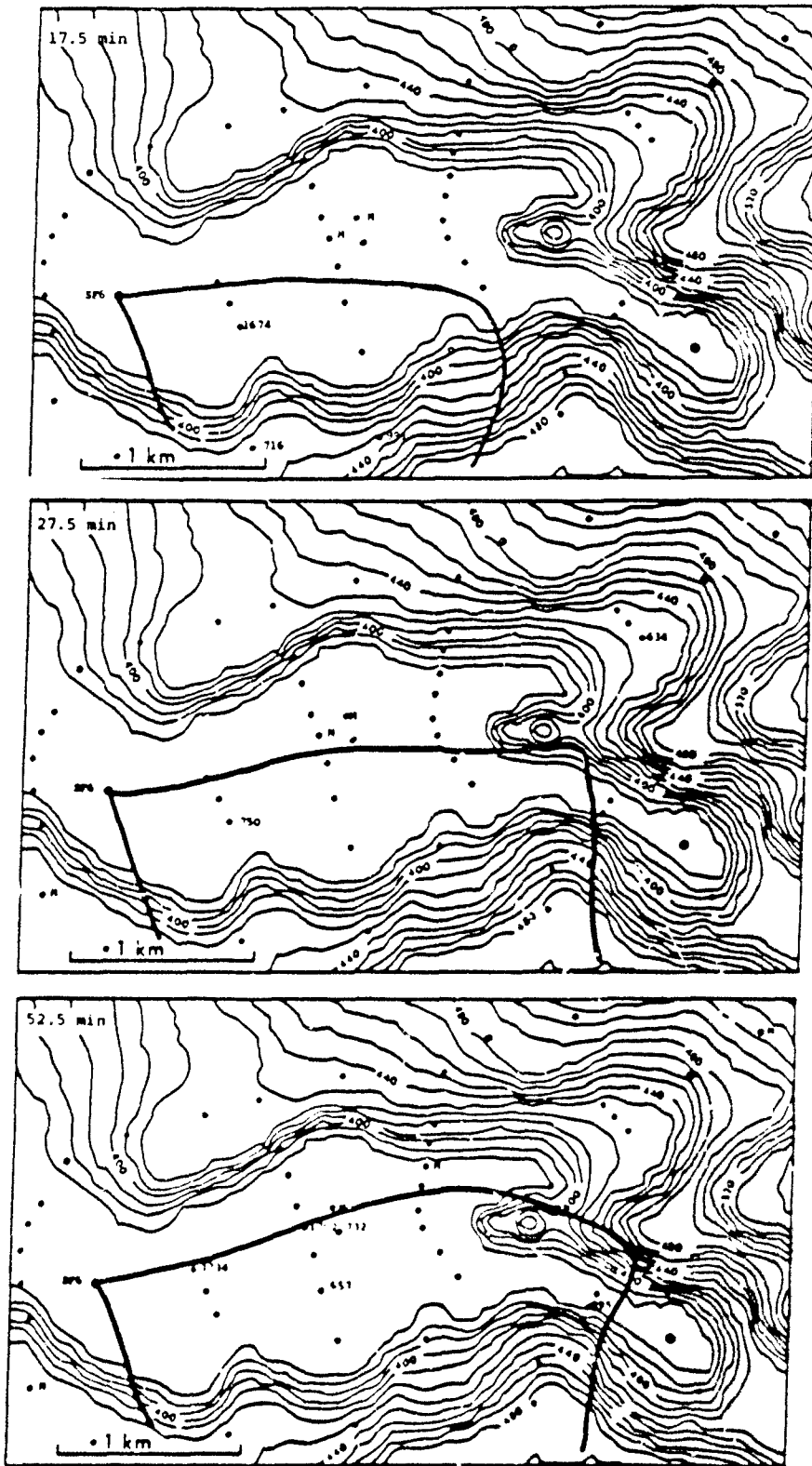


Figure 6. The WADOCT-derived 1000 PPT Concentration Line, and the Measured Concentration Values for the 5-min. Period Surrounding the Indicated Time. Results are for Test Number 6.



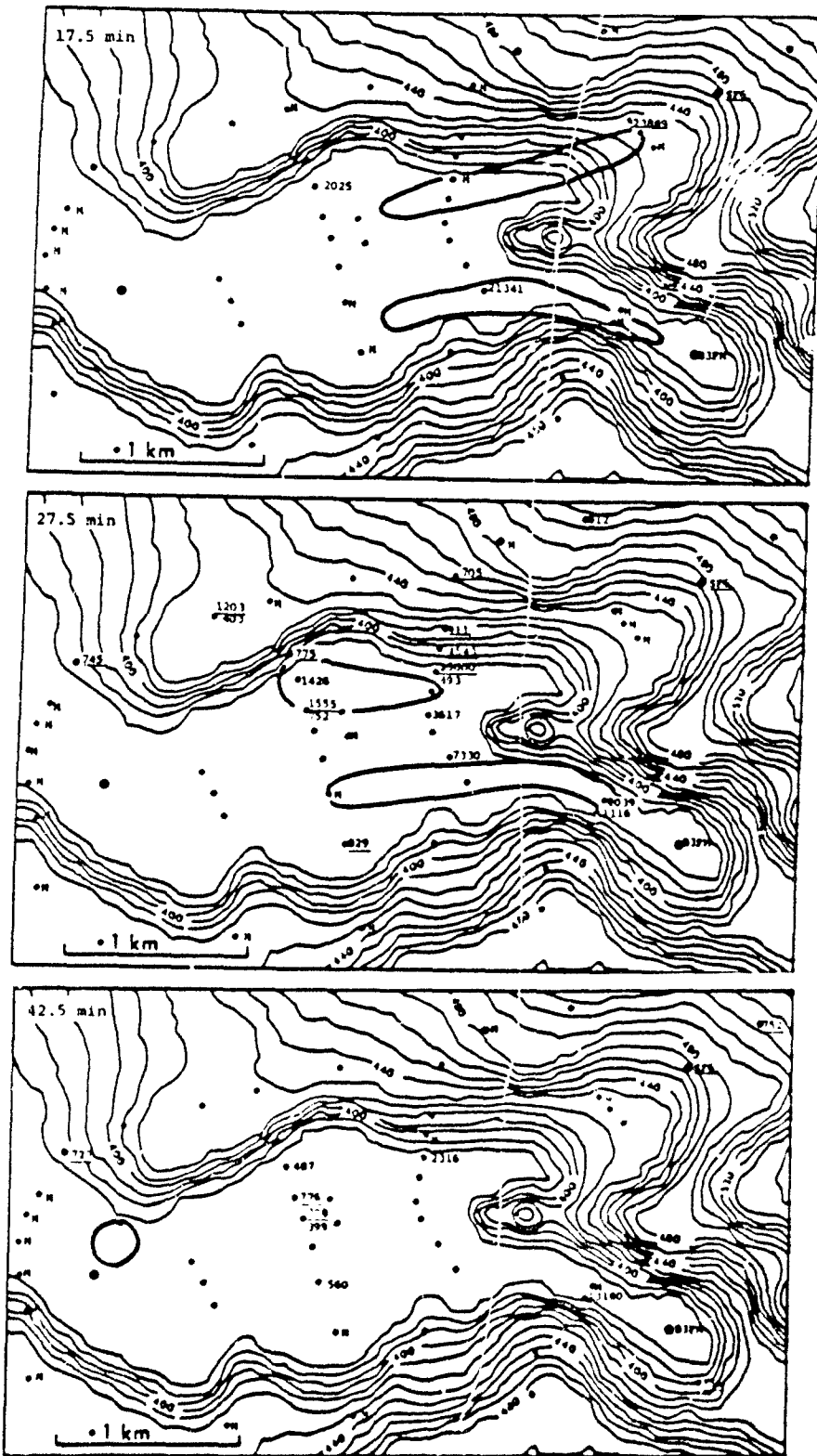


Figure 8. Same as Figure 7 Except for First Part of Test Number 8.





Figures 11 and 12 show the actual 1-hr mean plume and the model predicted plume for Tests 7 and 10, respectively. In the stable case (Test 7), the plume trajectories agree very well. However, the model predicts higher concentrations and greater distances than the observed. It is not clear how much of this difference is due to the sampler threshold problem stated above. In the unstable case (Test 10), the hazard distances agree quite well, but the model plumes are much broader than the actual plumes. For the SF<sub>6</sub> release, the model predicts a diverging windfield due to the unstable air being lifted up over the south wall of the valley. For the B3FM release, the model shows a diverging flow from the broad valley up into Paynes and Plum Creeks. Although the sampler data show that the bulk of the tracer went up Plum Creek, there were traces of B3FM detected in the Paynes Creek area.

Some general conclusions can be drawn from these analyses:

1. Short term measured concentrations (5-min) do not reflect a Gaussian distribution, and therefore, it is difficult to compare the Gaussian model calculations with the data unless averaged over several 5-min periods.
2. The model concentrations are of the same order of magnitude as the measured concentrations.
3. The model does a reasonable job at defining the general area of the plume, but does tend to overpredict the length and width of the plume.

## **4.2 Mountain Iron**

### **4.2.1 GENERAL**

Two problems exist in using the Mountain Iron data to evaluate models: 1) the samplers were not positioned in concentric arcs, and 2) the concentration data from each sampler is not available. The Mountain Iron reports do include the plume patterns for each test and a tabulation of the apparent centerline concentrations at various distances from the source. It was these two pieces of information that were used in evaluating the WADOCT model.

The only available tabulated wind data was that measured at the source. Wind data from other locations were plotted on the plume pattern figures, but were not used in the evaluation. Most of the plumes were reasonably straight, and therefore, it was decided that little would be gained by including other wind measurements in the WADOCT calculations.

Buoyancy and stability conditions were determined from the solar, sky, and wind conditions. Some runs were made using the standard deviation of wind direction but, overall, there was little difference in the computed distances.

The model contained a 56 x 61 array that covered most of the area shown in Figure 5. The grid spacing was 200 m. Surface roughness lengths were included in the array. The surface roughness varied from 0.1 cm over the water to 20 cm over the low lands near the water to 112 cm over the more rugged terrain.

Two types of analyses were conducted. One was simply comparing the WADOCT plume plots with those presented in the Mountain Iron report. The other type of analysis was a statistical evaluation using the data from all 87 tests.

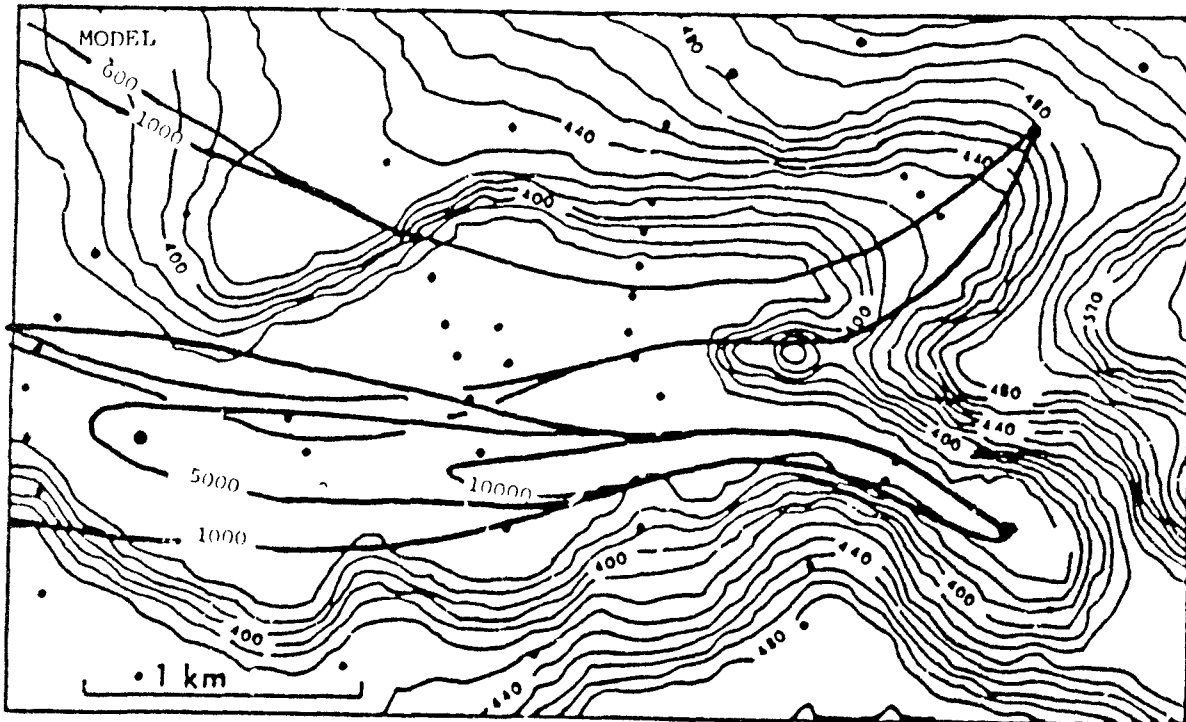
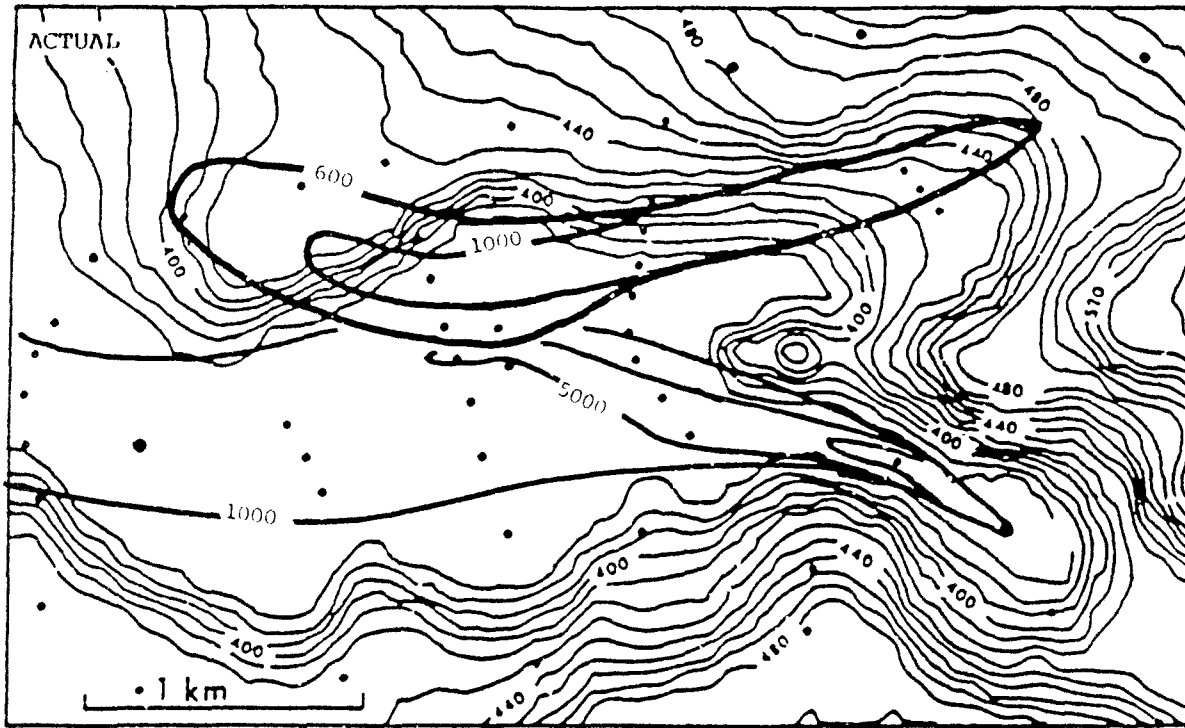


Figure 11. The 1-hr Mean Actual Plume and Model-derived Plume for Test Number 7. Contours are in PPT.

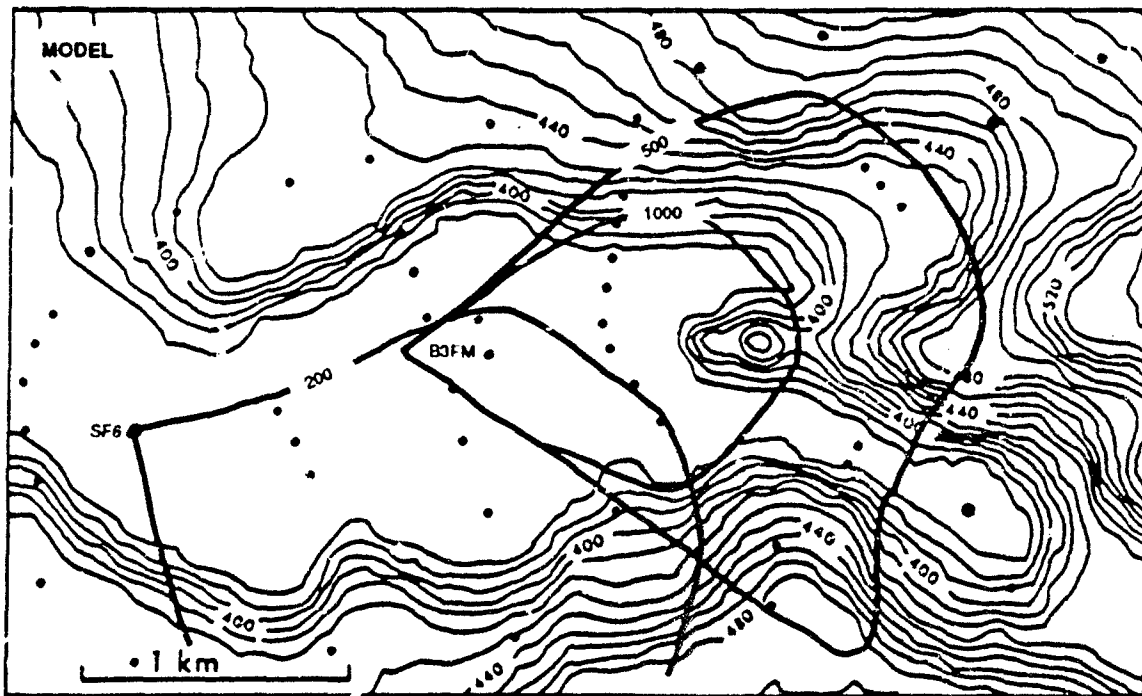
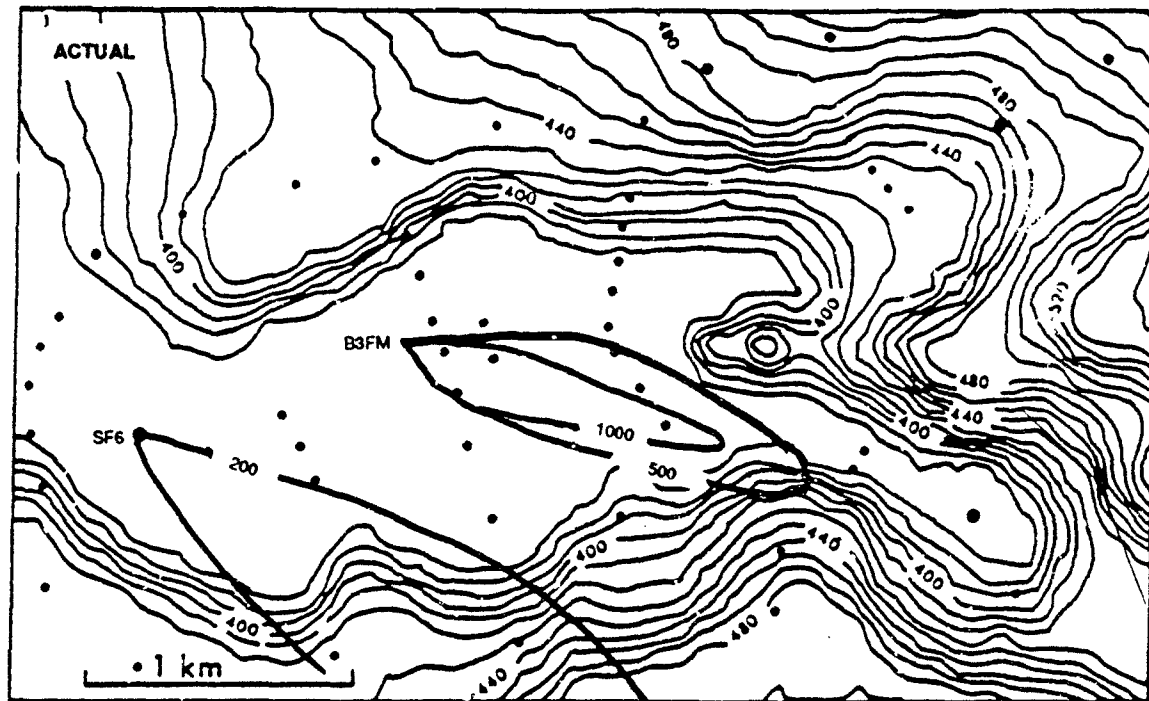


Figure 12. Same as Figure 11 Except for Test Number 10.

#### 4.2.2 PLUME COMPARISON

A comparison of the model-derived concentration contour plots and the actual contour plots from three cases are shown in Figures 13-15. These three cases were chosen because of the different wind directions, resulting in the plume traveling over terrain of varying complexities. The concentration contours shown in these figures are normalized concentrations,  $E/Q$ , ( $10^9 \text{ sec m}^{-3}$ ).

Figure 13 is a plot of Test 60, conducted at 1255 PST on 27 April 1966. The westerly winds advected the plume over a relatively flat area where the land rises gradually from sea level to about 200 m at a distance of about 6 km from the source. The observed and computed concentration distances agree reasonably well. The observed 100 contour is open-ended, due to the lack of samplers beyond 6 km. The computed plume is considerably broader than the observed plume.

In Test 81, shown in Figure 14, the winds were from a more common northwesterly direction. As a result, the plume traversed over a more complex terrain, the most prominent features being Target Ridge, Honda Canyon, and Honda Ridge. This type of flow, which is perpendicular to the ridges, produces a double maximum in the concentration contours, the maximums occurring at the ridge tops and the minimum occurring in Honda Canyon. It is quite apparent that the plume does not descend on the lee side of Target Ridge. Its centerline remains elevated, thus producing low concentrations on the canyon floor. WADOCT assumes that the plume centerline remains at ground level, thus making it impossible to produce a double maximum. The lengths of the 1000 and 500 contour lines agree well, but the computed 100 contour line is considerably longer than the measured. This difference may be partly due to the plume remaining aloft as it passes over the samplers along the south shore. Again, it appears that the computed plume is wider than the actual plume.

In Test 98, the winds are from a more northerly direction. This test was conducted in the early evening on 6 July during neutrally stable conditions. The windflow took the plume over the west end of Target and Honda Ridges where the maximum height is about 300 m. Again, we see the double maximum over the two ridges. In this case, the calculated plumes are considerably longer than the measured plumes. The Mountain Iron equation, an empirical equation derived from the Mountain Iron data, also produced greater distances than the measured, but not as great as the WADOCT model.

#### 4.2.3 STATISTICAL EVALUATION

The basic set of data from the 87 test releases that were used are as follows:

1)  $C/Q$ , the centerline exposure normalized to unit source strength, where  $C$  is the centerline time-integrated concentration, and  $Q$  is the mass of tracer released during the test period.

2)  $X_o$ , the downwind travel distance from the release source to an air sampler.

The number of paired sets of  $C/Q$  and  $X_o$  listed ranged from one to six sets for each test release and the total number of sets of data used was 304 for the 87 tests.

In the study that follows, the data from Source A came from 65 tests with 41 classed as day tests and 24 as night tests. The number of data sets involved were 136 for daytime and 106 for nighttime. The data from Source B came from 22 tests, three of which were classed as night tests. The number of data sets were 49 for daytime and 13 for nighttime.

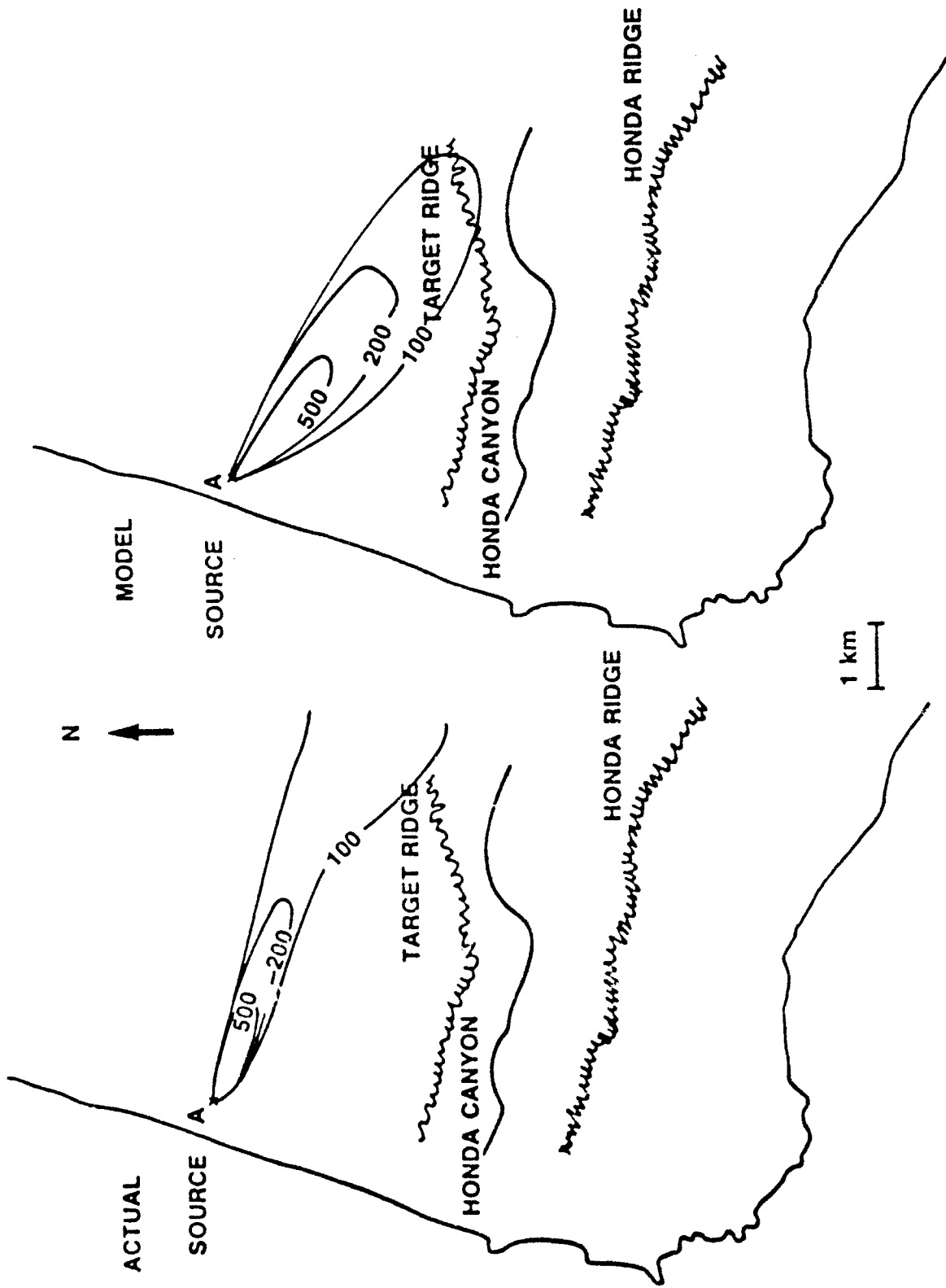


Figure 13. Actual and Model-Derived Concentration Contour Plots for Test Number 60, Conducted at 1255 PST on 27 Apr 66. Concentration Contours are Normalized Concentrations,  $C/Q$  ( $10^9 \text{ sec/m}^3$ ).

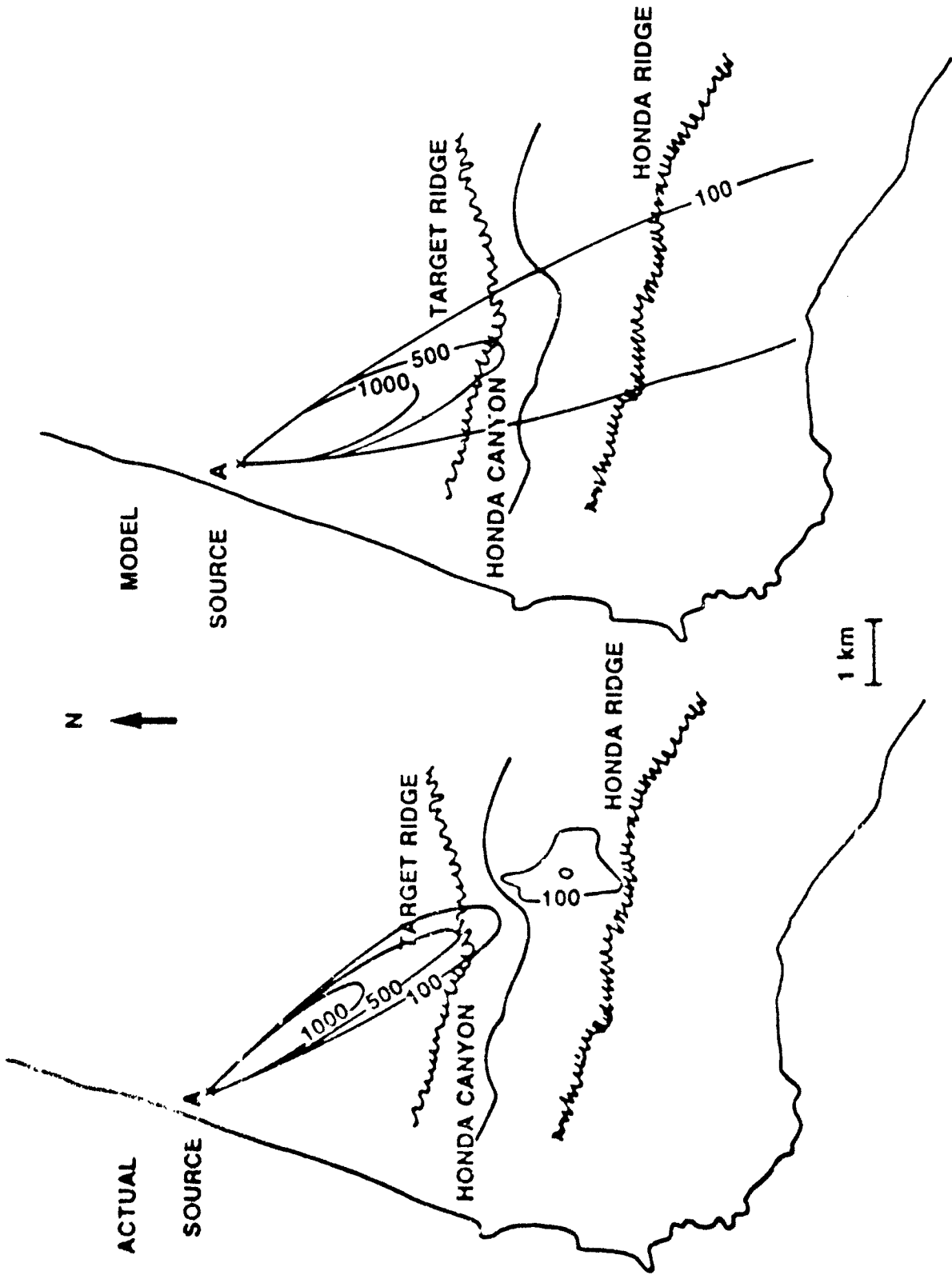


Figure 14. Same as Figure 13 Except for Test Number 81, Conducted at 2040 PST on 2 June 1966.

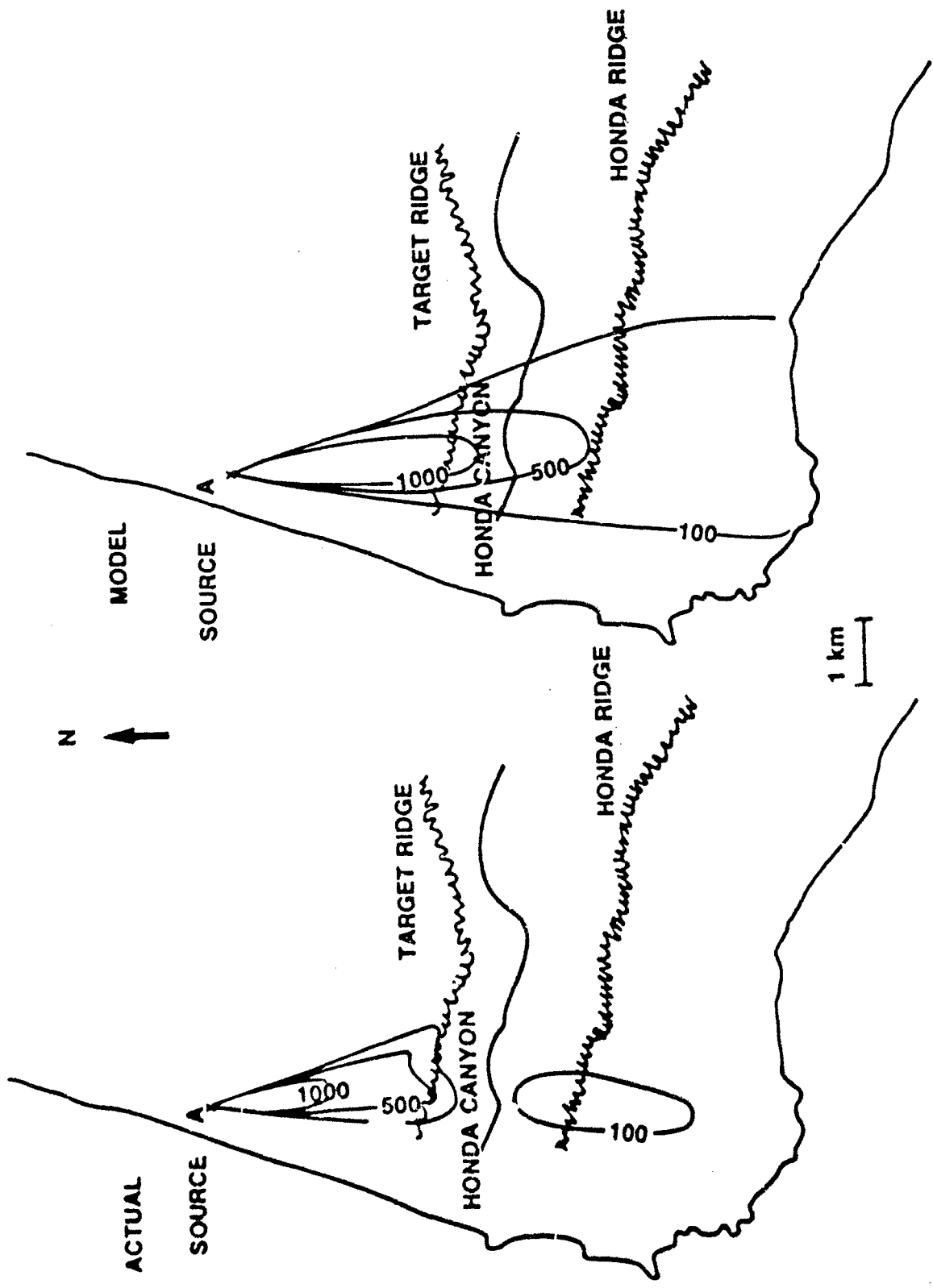


Figure 15. Same as Figure 13 Except for Test Number 90, Conducted at 1906 PST on 6 July 1966.

For the model calculations, a uniform wind field equal to the wind at the source was assumed. The primary reason for doing this was the long computation time involved in running the complete WADOCT model for the 87 cases. Most of the CPU time is used in the iteration process in adjusting the initial wind field to the final terrain-induced windfield. The nearly straight plume patterns shown in Reference 16 indicate a reasonably uniform wind field. The differences in the plume lengths, before and after adjusting to a relatively uniform wind field, are small and should not have an effect on the overall results and conclusions.

The calculated distances,  $X_c$ , are compared with the observed distances,  $X_o$ , in Figures 16 through 19 by separating the tests by sources and into day and night classes. The dashed lines represent the factor of two limits. The figures show that in 65 percent of the 304 data sets  $X_c$  was greater than  $X_o$ . Of those 63 percent, 58 percent overpredicted by a factor less than two and 96 percent by a factor less than four. Of the remaining 35 percent of the cases, 87 percent underpredicted by a factor less than two and all of them underpredicted by a factor less than four. Overall, the calculated distances fell within a factor of two of the observed distances 68 percent of the time, and within a factor of four 96 percent of the time. For the Source A releases only, the calculated distances fell within a factor of two 72 percent of the time, and within a factor of four 97 percent of the time. For the Source B releases the corresponding values dropped to 55 percent and 95 percent. The information in Figures 16-19 is summarized in Table 6. Also shown in Table 6 is the FB\* (Fractional Bias) which is an indication of whether the model tends to overpredict or underpredict the distance—a negative number indicating overprediction.

The Mountain Iron equation for Source A predicted the centerline concentration at a given distance within a factor of two 71 percent of the time, and within a factor of four 97 percent of the time. Since C is related to  $X^{-1.82}$  in the Mountain Iron equation, this translates to predicting the distance within a factor of 1.5 of the observed distance 71 percent of the time and a factor of 2.1, 97 percent of the time. This is considerably better than the WADOCT predictions.

Table 6. Percentage Distribution of Calculated vs Observed Distances by Source and Time of Day.

	SOURCE A			SOURCE B			TOTAL
	DAY	NIGHT	SUB TOTAL	DAY	NIGHT	SUB TOTAL	
NO. OF TESTS	41	24	65	19	3	22	87
NO. OF DATA SETS	136	106	242	49	13	62	304
$X_c > 4X_o$	1	6	3	2	15	5	4
$4X_o > X_c > 2X_o$	18	25	21	31	46	34	24
$2X_o > X_c > X_o$	34	41	38	37	31	36	37
$X_o > X_c > .5X_o$	40	28	34	22	8	19	31
$.5X_o > X_c > .25X_o$	6	0	3	8	0	6	4
$X_o < .25X_c$	0	0	0	0	0	0	0
FB*	-.27	-.67	-.49	-.14	-.52	-.21	-.45

\*FB is the fractional bias  $= (\bar{X}_o - \bar{X}_c) / |0.5(\bar{X}_o + \bar{X}_c)|$

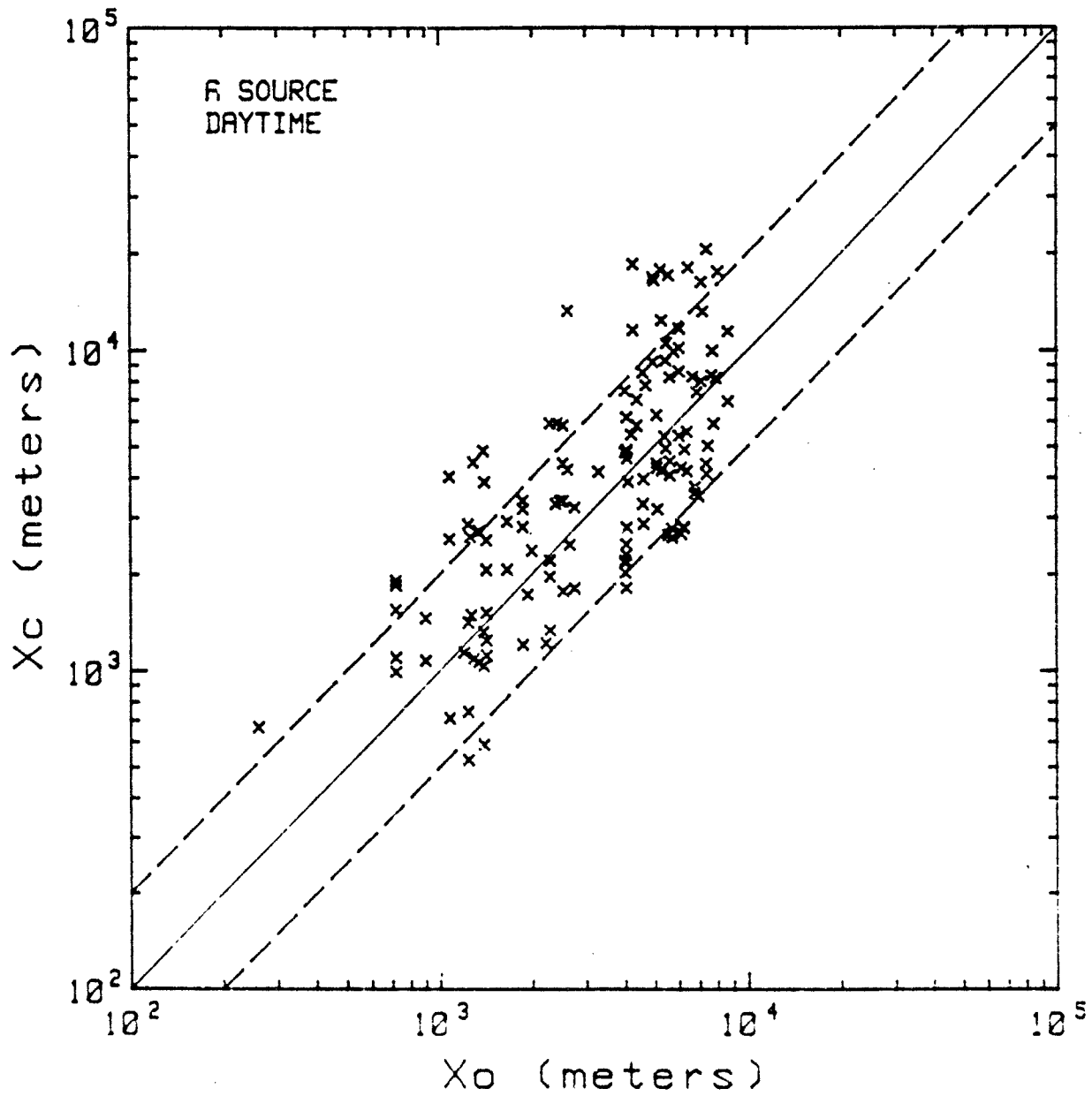


Figure 16. Scatter Plot of the Observed and Calculated Distances From Source A for Daytime Cases. Dashed lines are the Factor of Two Limits.

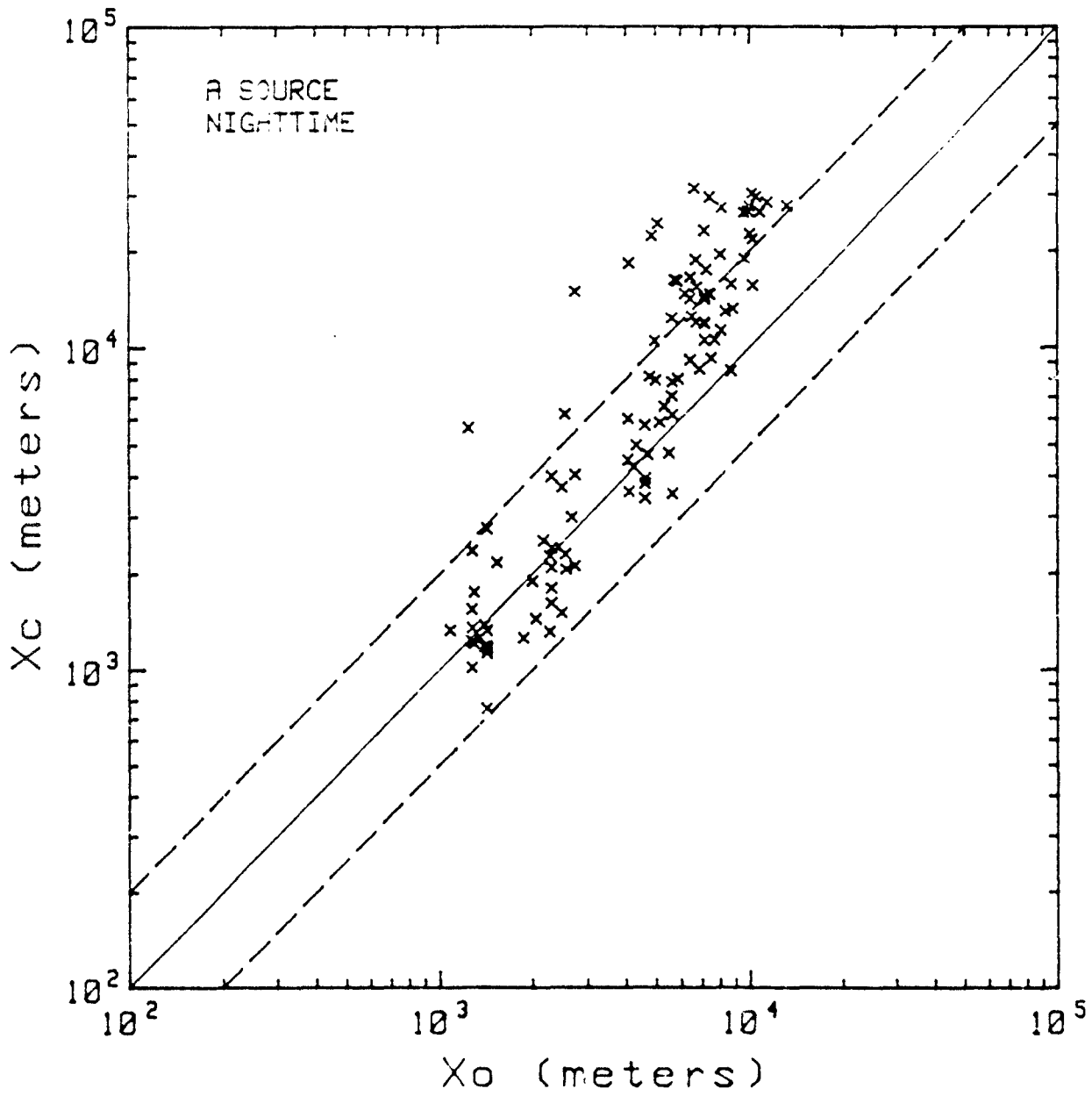


Figure 17. Same as Figure 16 Except for Nighttime.

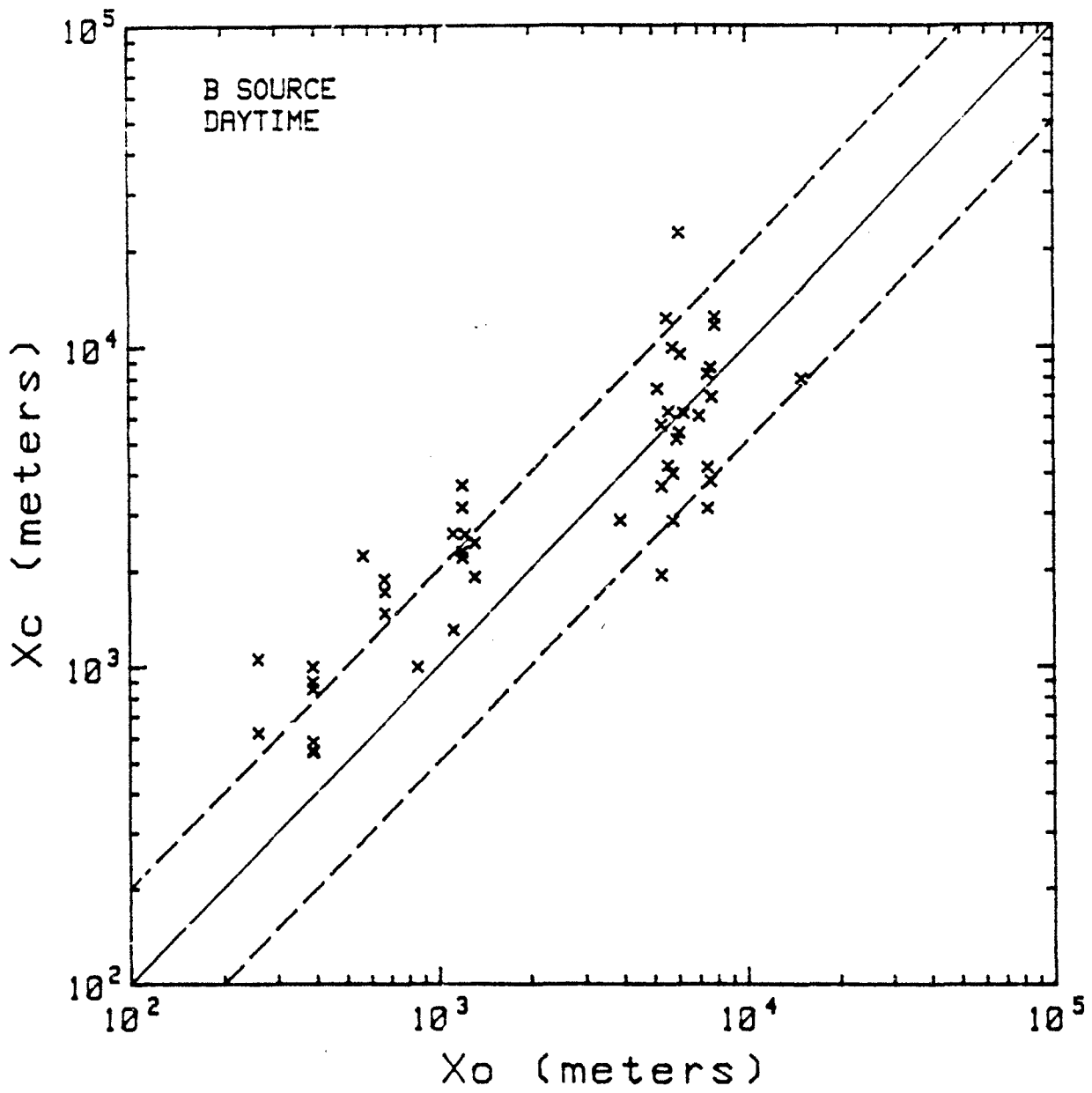


Figure 18. Same as Figure 16 Except for Source B.

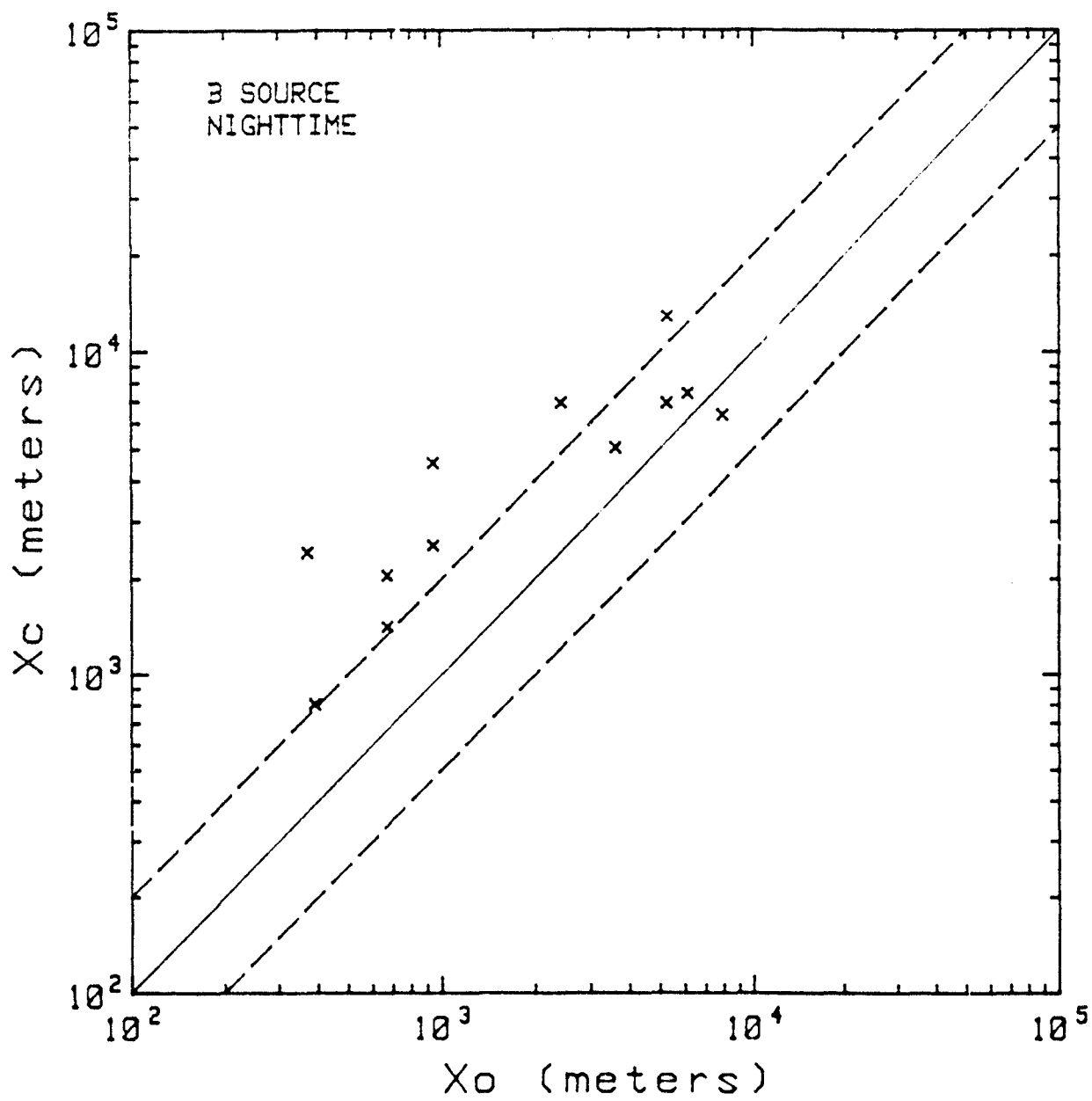


Figure 19. Same as Figure 16 Except for Source B and Nighttime.

## 5. CONCLUSIONS

The WADOCT model was evaluated using data from the AMADEUS and Mountain Iron diffusion experiments. The following is a list of some of the more important conclusions from this study.

1. The model does reasonably well in predicting wind direction but not wind speed.
2. Adjusting the atmospheric stability does not improve the overall accuracy of the windflow portion of the model.
3. The model adjusts the wind direction toward the actual streamlines but not completely.
4. Using an objective analysis scheme to initialize the wind data may produce worse results than initializing with a mean, uniform wind field.
5. In the AMADEUS results, using mean data from 10 stations produces slightly better results than using data from 4 of the 10 stations.
6. WADOCT tends to overpredict the distance and width of the plume. WADOCT overpredicted the distance in 65 percent of the Mountain Iron cases.
7. Since WADOCT assumes that the plume centerline remains at a constant height above ground, it is unable to reproduce the minimum concentrations that occur between Target and Honda Ridges.

The question of whether WADOCT should be used as an operational model can not be answered with a simple "yes" or "no". The big advantage of the WADOCT model is its ability to run on a microcomputer. The model can take several minutes of CPU time to run, especially when using a large grid, but with technology continually reducing the processing time, it is expected that the computation time for a microcomputer will not be a problem in a few years.

The ultimate decision, however, must be based on the model's ability to produce accurate dispersion footprints. A successful complex terrain dispersion model is one that performs well when the actual wind field shows a great deal of spatial variability due to the terrain. Unfortunately, under these conditions WADOCT will only partially adjust the wind field to the actual wind field, thus producing an error in the plume trajectory. The plume trajectory may be slightly better than when a uniform wind field is assumed, such as in AFTOX, but the slightly greater accuracy may not justify the additional time to input the data and run the calculations. When the actual windfield is reasonably uniform because of the terrain being relatively flat and/or the stability conditions being neutral, WADOCT performs well. However, there is little advantage to using a complex terrain dispersion model under these conditions.

By using a complex terrain dispersion model, one would hope to be able to more accurately predict the path of the plume and thus, narrow the width of the toxic corridor. However, with the uncertainty in WADOCT's ability to produce reliable wind directions, the toxic corridor width can not be reduced significantly over that defined by AFTOX.

One would also hope to be able to more accurately define the toxic corridor length. There are some differences in the lengths calculated by AFTOX and WADOCT. However, for the most part these differences are small relative to the effects that the uncertainties and approximations inherent in both models have on the toxic corridor length computation.

## References

1. Lanicci, J.M. (1985) *Sensitivity Tests of a Surface-Layer Windflow Model to Effects of Stability and Vegetation*, AFGL-TR-85-0265, ADA169136.
2. Lanicci, J.M., and Weber, H. (1986) *Validation of a Surface-Layer Windflow Model Using Climatology and Meteorological Tower Data From Vandenberg AFB, California*, AFGL-TR-86-0210, ADA 178480.
3. Lanicci, J.M., and Ward, J. (1987) *A Prototype Windflow Modeling System for Tactical Weather Support Operations*, AFGL-TR-87-0159, ADA 189362.
4. Kunkel, B.A. (1988) *User's Guide for the Air Force Surface-Layer Windflow Model (AFWIND)*, AFGL-TR-88-0157, ADA 208710.
5. Kunkel, B.A. (1988) *User's Guide for the Air Force Toxic Chemical Dispersion Model (AFTOX)*, AFGL-TR-88-0009, ADA199096.
6. USNRC (1972) *Onsite Meteorological Programs Regulatory Guide 1.23*, U.S. Nuclear Regulatory Commission.
7. Sedefian, L., and Bennett, E. (1980) A comparison of turbulence classification schemes, *Atmos. Environ.* **14**:741-750.
8. Cressman, G.P. (1959) An operative objective analysis scheme, *Mon. Wea. Rev.* **87**:367-374.
9. Golder, D. (1972) Relations between stability parameters in the surface layer, *Boundary Layer Met.* **3**:46-58.

10. Mitchell, A.E., Jr. (1982) A comparison of short-term dispersion estimates resulting from various atmospheric stability classification methods, *Atmos. Environ.* 16:765-773.
11. Fleischer, M.T. (1980) *SPILLS—An Evaporation/Air Dispersion Model for Chemical Spills on Land*, Shell Development Company, PB 83109470.
12. Clewell, H.J. (1983) *A Simple Formula for Estimating Source Strengths from Spills of Toxic Liquids*, ESL-TR-83-03.
13. Ille, G., and Springer, C. (1978) *The Evaporation and Dispersion of Hydrazine Propellants from Ground Spills*, CEEDO-TR-78-30.
14. Kunkel, B.A. (1983) *A Comparison of Evaporative Source Strength Models for Toxic Chemical Spills*, AFGL-TR-83-0307, ADA139431.
15. Clonco, R.M. (1989) *AMADEUS: A Dispersion Study Over Moderately Complex Terrain*, Preprint Volume of the 6th Joint Conference on Applications of Air Pollution Meteorology, Anaheim, Calif.
16. Hinds, W.T., and Nickola, P.W. (1967) *The Mountain Iron Diffusion Program: Phase I South Vandenberg: Volume I*, AFWTR-TR-67-1, AD 721858.
17. Hinds, W.T., and Nickola, P.W. (1968) *The Mountain Iron Diffusion Program: Phase I South Vandenberg: Volume II*, AFWTR-TR-67-1, AD 721859.